UNIVERSIDADE D
COIMBRA

Ana Teresa Brito Maduro

THE IMPACT OF THE DIET IN ADULT C57BI/6J MICE PANCREAS FUNCTION WITH AGE

Dissertação no âmbito do mestrado de Biologia Celular e Molecular, orientada pela Professora Doutora Raquel Soares, coorientada pela Professora Doutora Ana Luísa Carvalho e apresentada ao Departamento de Ciências da vida da Faculdade de Ciências e Tecnologia

Outubro de 2021

Departamento de Ciências da Vida da Faculdade de Ciências e Tecnologia
da Universidade de Coimbra

THE IMPACT OF THE DIET IN ADULT C57BI/6J MICE PANCREAS FUNCTION WITH AGE

Ana Teresa Brito Maduro

Dissertação no âmbito do Mestrado em Biologia Celular e Molecular orientada pela Professora Doutora Raquel Soares da Unidade de Bioquímica, do Departamento de Biomedicina, da Faculdade de Medicina da Universidade do Porto (FMUP)/Instituto de Investigação e Inovação em Saúde (i3s), coorientada pela Professora Doutora Ana Luísa Carvalho do Departamento de Ciências da Vida da Universidade de Coimbra e apresentada ao Departamento de Ciências da Vida da Faculdade de Ciências e Tecnologia da Universidade de Coimbra

Outubro de 2021

1 2 9 0

UNIVERSIDADE D
COIMBRA

The present study was performed in the Biochemistry Unity of the Biomedicine Department of the Medicine Faculty of the University of Porto, under supervision of Professor Doctor Raquel Soares, mentored by Carla Luís and under co-supervision of Professor Doctor Ana Luísa Carvalho from the University of Coimbra.

Acknowledgments

I would like to express my sincere, deep, and warm acknowledgments to my supervisor Professor Doctor Raquel Soares, who believed in me since day one and provided me with the opportunity to join her group. Without her trust, support, knowledge, and expertise this work would not be possible.

I want to express my gratitude to my mentor Carla Luís for always being there for me with ideas and suggestions to guide me through the obstacles that I had to face over the past year. Thank you for your help in the lab and your revising and encouraging comments along this work.

A special note of appreciation to my co-supervisor Professor Doctor Ana Luísa Carvalho, first for giving me the opportunity to study in this master, and for always being available to help whenever necessary.

I am deeply grateful to Anabela Silvestre for making me a "staining expert" and a "master in immunohistochemistry", as she used to call me. Thank you, for teaching me so much about histological procedures (and life too) and for being always ready to help me, even when you had a thousand things to do in that same minute. You are one of a kind.

I also want to thanks to the members of the *Metabasity Group*, from FMUP/i3s, particularly to Professor Doctor Susana Guerreiro and Raquel Costa, for their support and their readiness to help me.

I want to thank my friends Francisco and Adriana for their help and support, we were like a team and I really appreciate for had the opportunity to know you and to share with you some of the most incredible moments of this past year.

Also, Victoria Raísa, my eternal roommate, thank you for being my big sister during this year. You helped me to grow and to become the best version of myself.

To all my friends of F.R.I.E.NDS, Andreia, Leite, Bia, Carolina, Rodrigo e Rela, a warmly thank you for always believing me and supporting me. You guys are my safe haven, always.

Finally, I want to give my loving thanks with all my heart to my parents Belita e Carlitos. Thank you for always being there for me, fighting for me, and for making me the person that I am today. Without you, this work would never be possible.

Table of contents

List of figures

.

List of tables

Abbreviations

ROS	Reactive oxygen species
SA- β-gal	Senescence-associated- β-galactosidase
SASP	Senescence-associated secretory phenotype
$p16^{INK4A}$	Cyclin-dependent kinase inhibitor 2A
p53	Cellular tumour antigen p53
p21	Cyclin-dependent kinase inhibitor 1
Rb	Retinolasma protein
DDR	DNA damage response
ATM	Ataxia telangiectasia mutated
CDK	Cyclin depend kinase
GLB1	Galactosidase Beta 1
LB	Lipofuscin Bodies
PP-cells	Polypeptide-producing cells
T2D	Type 2 diabetes
ND	Normal diet
HFD	High-fat diet
FELASA	Federation of European Laboratory Animal Science
LDL	low-density lipoproteins
H&E	Hematoxilyn and Eosin
PAS	Periodic-acid-Schiff
Ca^{2+}	Calcium
UV	Ultraviolet
SBB	Sudan-Black-B

MT	Masson Trichrome
SR	Sirius Red
IHC	Immunohistochemical
PCNA	Proliferating cell nuclear antigen
PBS	Phosphate-Buffered Saline
PBS-T	PBS-Tween 20
BSA	Bovine Serum Albumin
ABC	Avidin-biotin complex
DAB	3, -3’diaminobenzidine
Tris-HCl	Tris-Hydrochloride
H_2O	Water
SEM	Standard error of the mean
IAPP	Islet amyloid polypeptide

Resumo

O envelhecimento é um processo biológico e multifatorial que gera uma progressiva deterioração de vários órgãos, resultando na disfunção dos tecidos. A obesidade é uma condição metabólica que afeta o metabolismo de vários tecidos, de forma semelhante ao envelhecimento, uma vez que induz o desenvolvimento prematuro do estado de senescência das células. O pâncreas é um dos tecidos mais afetados pela ingestão excessiva de nutrientes, levando à disfunção das células β pancreáticas.

Estudos anteriores, onde se abordou o efeito da obesidade nas consequências relacionadas com o envelhecimento no pâncreas, sugerem que a disfunção das células β, em ratinhos e humanos obesos e novos, se deve à sua entrada prematura em senescência. Por outro lado, em estudos recentes observou-se uma relação inversa entre a obesidade e os danos no fígado e no tecido adiposo de ratinhos obesos em idade adulta e em idade avançada.

Neste projeto de investigação, nós pretendemos avaliar os efeitos da obesidade induzida pela dieta nas consequências relacionadas com a idade no pâncreas de ratinhos adultos, ao longo do tempo.

Assim, ratinhos da estirpe C57Bl/6J sujeitos a uma dieta *standard* e a uma dieta rica em gordura foram monitorizados durante 12, 16 e 20 semanas, com a avaliação da morfologia do pâncreas, da expressão de insulina pelas células β, da acumulação de glicogénio no pâncreas, da deposição de cálcio e do conteúdo em células senescentes e em fibrose. Os resultados para o grupo sujeito a uma dieta *standard* elucidam para uma alteração na função pancreática, especialmente das células β, com um aumento de células β senescentes seguido por uma diminuição da produção de insulina e um aumento da fibrose no pâncreas dos ratinhos, ao longo período do estudo. Relativamente ao grupo sujeito a uma dieta rica em gordura, os parâmetros avaliados mostraram uma desregulação da função pancreática às 16 semanas, altura em que é atingida a obesidade, com atenuação dessas consequências metabólicas nos pâncreas dos ratinhos mais velhos. Com este estudo, nós sugerimos que há uma proteção metabólica no pâncreas de ratinhos mais velhos.

Palavras-Chave: Envelhecimento, obesidade, pâncreas, células β, senescência celular

Abstract

Ageing is a multi-factorial biological process that generates progressive deterioration across multiple organs, resulting in tissue dysfunction. Obesity is a metabolic condition associated with a metabolic impairment in many tissues, resembling ageing, by inducing premature cellular senescence. Pancreas is one of the mainly tissues affected by an exceeded nutrient intake, leading to islets β-cell dysfunction.

Previous studies regarding the obesity age-related consequences in pancreas suggest the induction of premature cellular senescence to explain pancreatic β-cells dysfunction in young obese mice and humans. On the other hand, recent studies observed a reverse of the obese deleterious effects in liver and adipose tissue in obese middle and advanced-age mice.

In this research project, we aimed to evaluate the effects of diet-induced obesity in the age-related pancreatic features in adult mice, with time.

Thus, C57BI/6J mice under a *standard* diet and under a high-fat diet (HFD) were monitored during 12, 16 and 20 weeks, and pancreas morphology, β-cell insulin expression, pancreatic glycogen accumulation, calcium deposits, cellular senescence, and fibrotic content were evaluated. The results for the *standard* diet group elucidate an alteration in the pancreatic function, especially for β-cells, along to the period of the study, with an increase in β-cells senescence followed by decreased insulin production and increase fibrogenesis. Regarding the HFD group, the evaluated parameters show an impairment in pancreatic function at week 16, time where obesity is reached, with an attenuation of these pancreatic metabolic features at the advanced age. Here we suggest a metabolic protection in obese adult mice pancreas at advanced ages.

Keywords: Ageing, obesity, pancreas, β-cells, cellular senescence

1. Introduction

1.1 Ageing

Physiological ageing includes a progressive loss of the tissue and organ well function, over time[1]. Recently, ageing research has experienced an unprecedented advance, particularly with the discovery that the rate of aging is controlled, at some point, by genetic pathways and processes conserved in evolution[2].

Some cell mechanisms are identified as ageing hallmarks in the majority of the tissues. Genomic instability, telomere attrition, epigenetic alterations, loss of proteostasis, deregulated nutrient-sensing, mitochondrial dysfunction, stem cell exhaustion, altered intercellular communication, and cellular senescence are the major aging hallmarks (*Figure 1*)[3]. This latter one is considered to be the key factor in the complexity of this biological process[4].

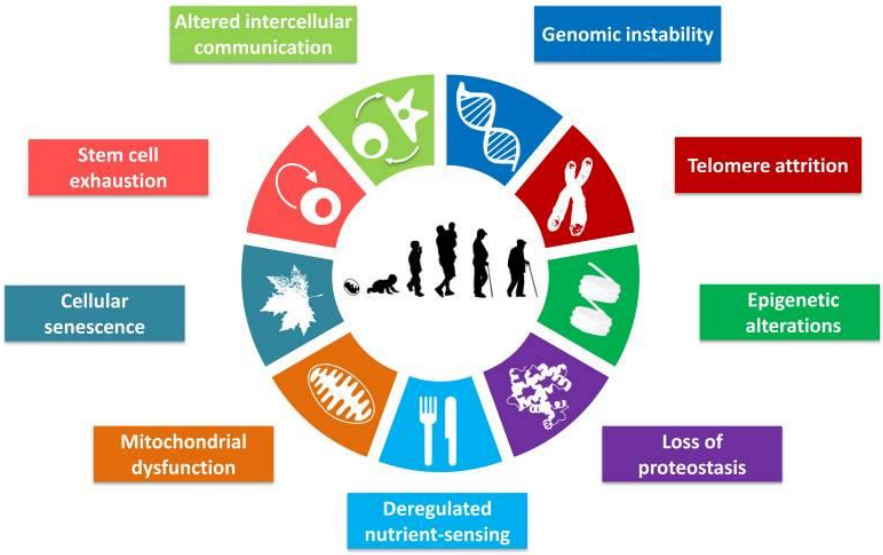

Figure 1. **Ageing Hallmarks**. This scheme exhibits all the hallmarks of ageing that were identified until now: genomic instability, telomere attrition, epigenetic alterations, loss of proteostasis, deregulated nutrient-sensing, mitochondrial dysfunction, cellular senescence, stem cell exhaustion, and altered intercellular communication[3].

1.1.1 Cellular Senescence

Hayflick and Moorhead (1961) were the first researchers identifying senescent cells, during serial passage of human fibroblasts. Cellular senescence is also described for other cell types, namely, epithelial and endothelial cells, lymphocytes, and in post-mitotic cells, like neurons or glial cells[5].

Evidence for both physiological and pathological cellular senescence can be achieved. Senescence has an important role during development and is essential for tissue remodelling[6]. In previous studies it was observed that senescence can be engaged during wound healing and contributes to its resolution[7]. Also, senescence-induced in tumour cells is being used as a potent anticancer mechanism[8]. Nonetheless, senescent cells accumulation in the tissues can negatively affect its regenerative capacity and create a proinflammatory milieu favourable for the onset and progression of age-related diseases as cardiovascular diseases, neurodegenerative disorders, cancer, and metabolic syndrome[9,10].

Senescent cells are characterized by a cell cycle division arrest in response to different damaging stimuli, mainly, reactive oxygen species (ROS) formation[11], telomere shortening[12], activation of cyclin-dependent kinase inhibitors as p16 and p21[13], increased activity of the senescence-associated β-galactosidase (SA- β-gal) enzyme[14], and lipofuscin accumulation[15], which will involve a metabolic reprogramming (*Figure 2*). Contrary to apoptosis, in which phagocytes are released to remove damaged cells without inflammation development, senescent cells survive as a result of the senescence-associated secretory phenotype (SASP) activation[16].

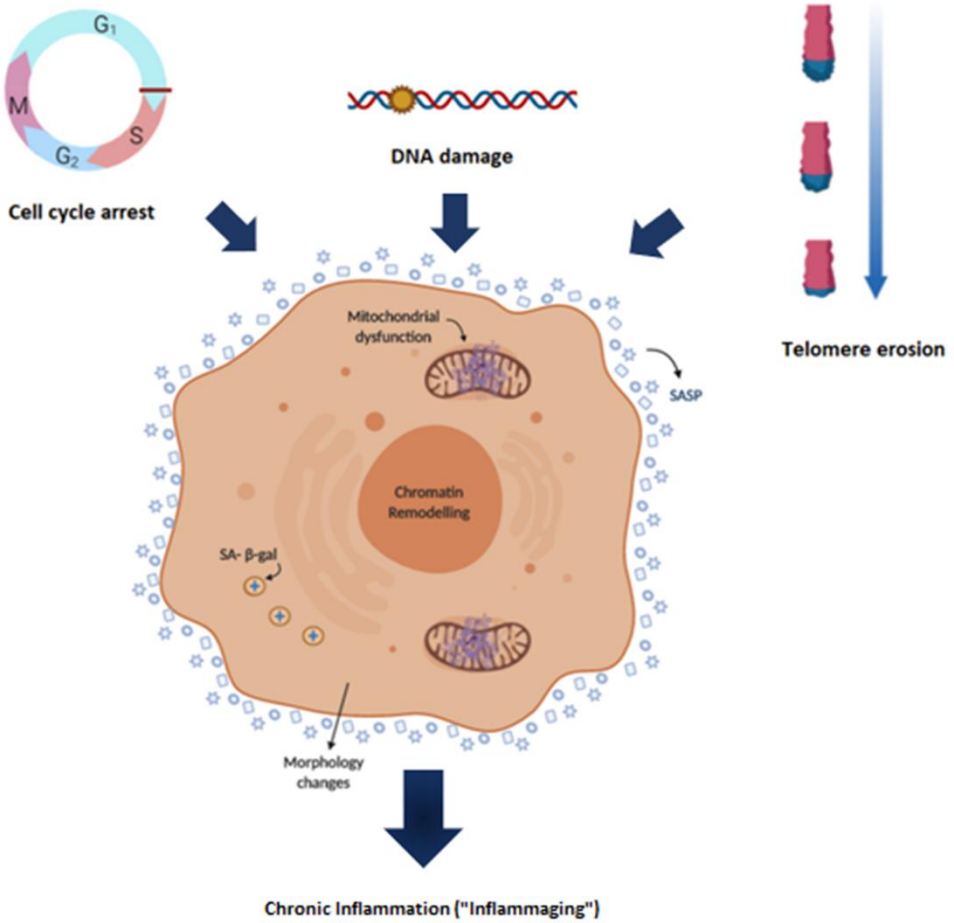

Figure 2. **Cellular senescence activation.** Senescence can be initiated by various stimuli that will lead to the p53/p21 and $p16^{INK4A}$/Rb pathways activation, resulting in an irreversible cell cycle arrest. Initially, senescent cells are identified by chromatin remodelling and telomere erosion. Senescent cells are characterized for the release of various molecules, including chemokines, cytokines, growth factors, and others, determining senescence-associated secretory phenotype (SASP). There is also an increase in mitochondrial metabolism and resistance to apoptosis. Further alterations related to the ageing process and long-lasting cellular damage will interfere with the normal phenotype of the cell and extend chronic inflammation.[12]

1.1.1.1 Oxidative stress

ROS are natural by-products of normal oxygen metabolism, considered essential to regulate several physiological functions as signal transduction, gene expression, and proliferation. However, with age, the balance between oxidant generation and the antioxidant processes in the tissues is disrupted, causing an increase in ROS production and its accumulation, leading to damage in macromolecules as DNA, proteins, and lipids[17].

Endogenous or exogenous sources of ROS, stimulate the cellular senescent phenotype by negatively affecting mechanisms involved in the response to DNA damage and epigenetic regulation, and activating tumour suppression pathway, including p53, p21 and Rb[18].

Together with the SASP factors, ROS stimulate a positive feedback loop, which will increase the demand for ROS production, especially mitochondrial ROS, increasing intracellular ROS content and contributing to the maintenance of the senescent phenotype by telomere shortening and dysfunction[19].

1.1.1.2 Telomere shortening

Telomeres are highly repetitive DNA specialized structures located at the end of chromosomes, composed of several kilobases (kb) of simple repeats (TTAGGG)n. They have the biological function to protect the chromosomes from end-to-end fusions, harmful rearrangements, and chromosome loss[20]. The length of telomeres is intimately related to the replicative ability of cells, characteristic that make them a used predictor of cellular senescence. DNA polymerases cannot synthesize DNA without a template, and the end-replication problem in telomeres is a consequence of this. This means that telomere shortening occurs in every cell cycle division[21]. In youth, the estimated length of the human telomeres is around 11 to 15kb and about 4 to 7kb in the elderly[22].

During normal ageing, the shortening of the telomeres is controlled by the telomerase. However, under some pathological conditions, there is an imbalance between telomere shortening and the counteracting by telomerase, resulting in accelerated senescence[23].

1.1.1.3 Tumour suppressors and cell cycle inhibitors

$p16^{INK4A}$, p53, and p21 are considered tumour suppressors and cell cycle inhibitors. The activation of this pathways occurs during senescence and is triggered by DNA damage. Telomere shortening can trigger a permanent DNA damage response (DDR) leading with the recruitment of the damage sensor ataxia telangiectasia mutated (ATM) to uncapped telomeres and resulting in upregulation of p53 and the p53 transcriptional target p21. In this setting, p21 inhibits cyclin-dependent kinase 2 (CDK2)-mediated inactivation of RB, preventing cells to enter the S phase of the cell cycle. DNA damage by oxidative stress can also support the ATM-p53-p21 axis.

Another barrier to proliferation is $p16I^{nk4a}$, which prevents CDK4- and CDK6-mediated inactivation of RB, resulting in cell cycle arrest. Depending on stress or cell type, this mechanism can act either alone or in combination with the p53-p21 pathway[13].

1.1.1.4 SA- β-gal activity

β-galactosidase is a lysosomal enzyme that hydrolyses β-galactosidases into monosaccharides and whose activity can be detected at pH 4.0. SA-β-gal is a distinct form of β-galactosidase that is expressed by senescent cells and whose activity can be detectable at pH 6.0. SA-βgal activity is strongly associated with senescent cells, since it is not detectable in quiescent cells or terminally differentiated cells, although a few exceptions can be noted[14].

Until a few years ago, it was unclear if SA-β-gal was a distinct enzyme that was induced by cellular senescent profile and that was only activated at pH 6.0 or whether if it was a consequence of altered expression/ activity of the regular lysosomal β-galactosidase.

Previous studies, observed that senescent cells had an increase number of lysosomes and an elevated lysosomal activity[24]. Recently it was verified that the SA-β-gal activity was due to an increase in the abundance of the β-galactosidase enzyme, result of an increase in expression of *GLB1* (Galactosidase beta 1) expression, the gene encoding for the classic lysosomal enzyme[25].

The SA-β-gal is often used as a biomarker of cellular senescence *in vivo* and the SA-β-gal activity assay is been widely used as a biomarker in studies of cellular senescence in both cultured cells and in freeze tissues[26,27].

1.1.1.5 Lipofuscin

Lipofuscin or the lipofuscin bodies (LB) consist in a fluorescent complex mixture composed by highly oxidized cross-linked macromolecules (sugars, proteins and lipids) with multiple metabolic origins. Because of its polymeric and highly cross-linked nature, LB cannot be degraded, accumulating within the lysosomes and cell cytoplasm of long-lived post-mitotic and senescent cells. In contrast, proliferative cells efficiently dilute LB aggregates during cell division, displaying very low levels or even no accumulation of this pigment[28].

Previous studies, verifies that in LB aggregation was present in senescent cells of aged tissues, suggesting that this can be a complementary senescent marker to look at with the SA-β-gal activity assay[29,3031,]

1.2 Pancreas and its age-related changes

Pancreas is a vital organ, with both endocrine and exocrine functions, which plays a crucial role in food digestion and glucose metabolism. Exocrine pancreatic cells represent about 85% of the total pancreas and are arranged in acini, small rounded clusters of secretory cells which empty into ducts, and have zymogen granules, functional units for synthesis, storage, and secretion of digestive enzymes. A much smaller percentage (about 2%) of the overall pancreatic gland mass is comprised of endocrine cells, which form the well-known, islets of Langerhans. At least four types of endocrine cells can be distinguished in pancreatic islets: α-cells, glucagon-producing cells, β-cells, which produce insulin, δ-cells, somatostatin-producing cells, and F-cells or pancreatic polypeptide-producing PP-cells (*Figure 3*)[32]. Of these, β-cells make up 60%-80%, of the islet cell population, and their dysfunction may result in sustained hyperglycaemia and consequently diabetes[33].

With ageing, it is observed a decrease in pancreas homeostatic capacity with a shrink in pancreas volume and an increase in the mean diameter of the pancreatic duct[34,35,36]. As illustrated in *Figure 4*, the incidence of fatty replacement, known as lipomatosis, and fatty infiltration increases with advancing age, which will lead to a gradual loss of exocrine tissue[37]. Lymphocyte infiltration is often found in older subjects and is related to the formation of chronic fibrosis[38].

The fibrotic content will increase around the acini, islets, and extracellular matrix, which contributes to the disruption of the acini structure and normal islets architecture and will lead to acini atrophy[39].

Differences in mice and human age-related changes in the islet cells are observed. In humans' subjects a decrease in the islet size and number was observed, due to loss of β-cells with ageing; whereas in mice, previous studies show an increase in islet sizes with unchanged islet number[40,41]. Also, the aged-human pancreas presents amyloid deposits in islets and vascular walls[42]. However, these were not described in murine pancreas.

Evidence suggests that the normal ageing process reduces the capacity for β-cells neogenesis or proliferation, in both rodents and humans[43,44].

Regarding the endcrine function, it is suggested a decrease in both basic β-cells insulin secretion and the secretion after glucose stimulation in older mice and humans, which reveals an impairment in insulin tolerance with ageing[45].

Decreased insulin secretion in ageing, owing to pancreatic cell dysfunction, has been associated with increased oxidative stress, endoplasmic reticulum stress, mitochondrial damage, inflammation, and β-cell deteriorated replication, which are common characteristics of cellular senescence[46,47]. Another characteristic observed in both aged pancreas and senescent cells is the accumulation of lipofuscin. Age-related accumulation of lipofuscin was detected in β-cells of humans, rhesus monkeys, and mice[48,49]. Finally, previous studies report the increased expression of the senescence effector $p16^{INK4A}$ in pancreatic islets during normal ageing in mice[50]. On these basis, it is been suggested that pancreatic β-cells dysfunction, which is observed in metabolic disorders for instances, occurs through the induction of β-cell senescence[51].

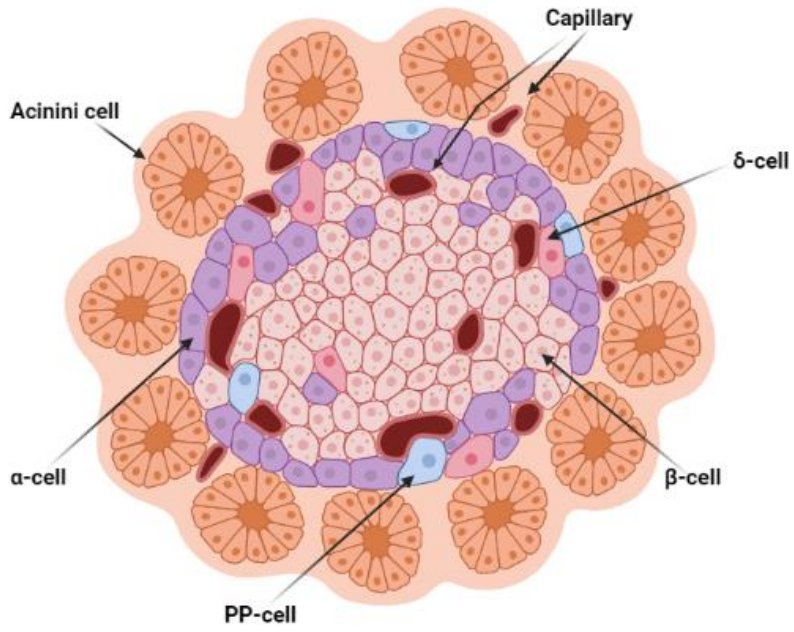

Figure 3. Representation of pancreatic islet of Langerhans surrounded by acini cells. Acini have an important role in the synthesis, storage, and secretion of digestive enzymes. All the four types of cells forming the pancreatic islets secrete different hormones that have an important role in the homeostasis of the metabolism. β cells (beta-cells) secrete insulin, important for the regulation of the glucose levels in the blood; α-cells (alpha cells) secrete glucagon, which promotes a critical response to hypoglycaemia situations; Δ-cells (delta-cells) secrete somatostatin, that blocks the secretion of both insulin and glucagon from adjacent cells; and PP-cells (polypeptide-producing cells), which regulates the pancreatic secretion activities. Image created in BioRender.com

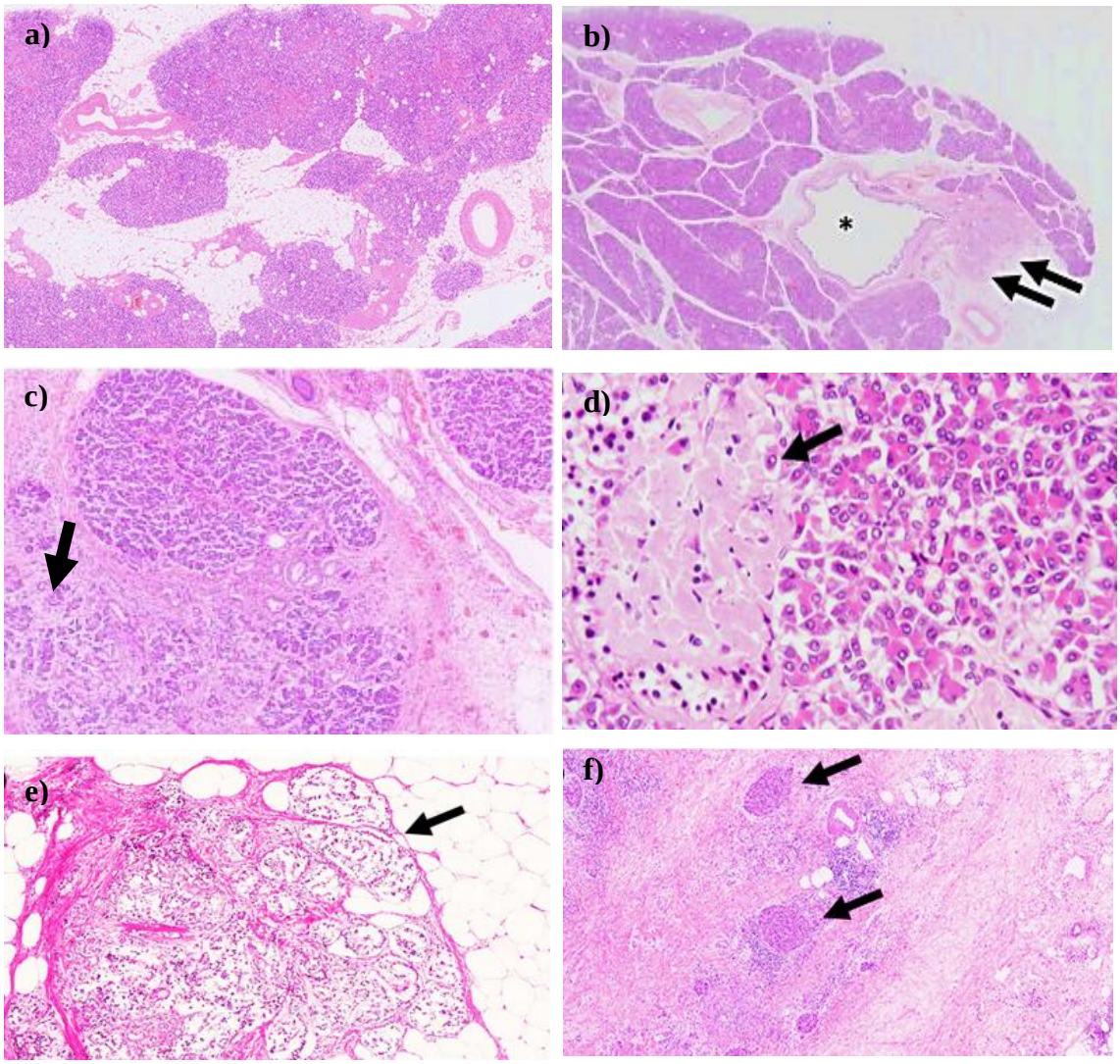

Figure 4. Morphological age-related changes in the pancreas. (**a**) Fat cells scattered within the atrophic pancreas. Images showing lobulocentric atrophy (arrow, **b** and **c**). Islet amyloid deposition (arrow, **d**). Aggregation of islets cells (arrow, **e**) within fat tissue, and islet cells (arrows, **f**) within fibrous tissue[52].

1.3 Obesity

Obesity is a condition of abnormally increased body fat, resulting from an unbalance between energy intake and energy expenditure[53]. Excessed body weight and increased plasmatic glucose, cholesterol, and lipoproteins levels are characteristics for both obese human and mice models[54]. The prevalence of obesity is rising worldwide, nowadays, and is considered to be a major risk factor for chronic diseases, including, type 2 diabetes (T2D)[55], which in turn ends up in increased morbidity and mortality rates worldwide, with high costs for the national health systems.

In the past few years, the decrease in lifespan of obese subjects has been associated with the development of cellular mechanisms also observed as well in the ageing process[56]. As a matter of fact, researchers have observed that excess nutrient intake can promote a premature induction of cellular senescence in many tissues, by accelerating intrinsic age-related causes of the senescent process. For example, increased metabolic loading is associated with mitochondrial dysfunction in the skeletal muscle[57]. Also, increased markers of ROS damage have been found in samples of adipose tissue, cardiovascular tissue, and liver of obese humans and mice[58], and pancreas is no exception. Obesity is also associated with cellular metabolic changes, including glucose uptake and the activation of the biosynthetic pathways, which can promote the activation and maintenance of the senescent state of the cells[12].

1.4 Effects of obesity in pancreas

Obesity caused by an excess of nutrient intake is associated with an increase in the plasmatic glucose levels. This will lead to an increase in insulin production by pancreatic β-cells, to prevent sustained hyperglycaemic levels, and the development of T2D.

One of the main characteristics described for both obese rodents and humans is an increase in the number and enlargement of islets caused by hyperplasia and/or hypertrophy of pancreatic β-cells. This is followed by an increase in blood insulin content (hyperinsulinemia), which precedes the complications of insulin resistance[59]. In T2D there is a decrease in islet mass, due to β-cell apoptosis, leading to insufficient insulin production[60].

Also, adipocyte infiltration and exocrine lesion of cell atrophy in both obese rodent and obese human pancreas was observed, associated with fibrosis located at the endocrine-exocrine interface, which could be associated with β-cell dysfunction[61].

Studies using mice subject to high-fat fed diet reveal an increase in markers of cellular senescence in β-pancreatic cells. An increase in SA- β-gal and significantly lower Ki-67 (proliferation marker) staining in high-fat diet-induced diabetic mice compared with control-fed counterparts was observed[60]; also it was suggested that $p16^{INK4a}$-induced senescence limits compensatory β-cell proliferation in response to metabolic loading, contributing to T2D[62].

However, none of these studies elucidates about the role of β-cells senescent state in obese non-diabetic mice.

1.5Aims

We start to age, right after we are born. Diet was observed to play a significant role in the cellular processes involved in ageing. Obesity has become a severe and worldwide health problem, especially in adult population, but its cellular and molecular features in the pancreas along time are not fully understood. Data on age-related changes in obesity has led some researchers to postulate that obesity could be considered a condition of premature metabolic dysfunction resembling ageing. This means that, for example, the changes that are observed in the pancreas of "healthy" older subjects will appear in younger obese subjects.

Yet, there are a few studies regarding the cellular and metabolic changes particularly in the pancreas tissue along with age and in high-fat diet conditions. Also, the available studies only look at the consequences of high-fat ingestion in young and very old animals, i.e., do not monitor pancreatic cellular changes with time. Additionally, they do not evaluate the cellular changes in the total pancreas and β-cells in both obese and diabetic conditions.

Thus, in this experimental study, we intend to:

- Evaluate the impact of the diet in the senescent state of mice pancreas during 12, 16 and 20 weeks;
- Evaluate the morphological changes in the exocrine and endocrine pancreatic cells of normal diet (ND) and high-fat diet (HFD) mice during 12, 16 and 20 weeks;
- Confirm the changes in insulin production for the ND and HFD groups during 12, 16 and 20 weeks;
- Access the pancreatic glycogen accumulation for both dietary groups during 12, 16 and 20 weeks;
- Evaluate the Ca^{2+} accumulation in the ND and HFD mice pancreas during 12, 16 and 20 weeks;
- Verify the proliferative state of the pancreatic cells for both dietary groups during 12, 16 and 20 weeks;
- Evaluate the fibrotic content in ND and HFD mice pancreas during 12, 16 and 20 weeks;
- Study the amyloid deposits formation in pancreas of the two experimental groups during 12, 16 and 20 weeks;

2. Material and Methods

2.1 Animal Studies

Experiments were performed in accordance with the Portuguese law on animal welfare and to the guidelines issued by the Federation of European Laboratory Animal Science Association (FELASA).

Six-weeks old male and female C57BI/6J mice (Charles River Laboratories Inc., USA) were housed in cages, at room temperature of 23± 5ºC and 35 ± 5% of humidity, with 12 h-dark photocycle (ZT0 as light onset and ZT12 as light offset). The animals had *ad libitum* access to water and food. The nutritional parameters as water and diet consumption, body weight, cholesterol, lipoproteins and glycaemic levels were measured once a week during the experimental study.

2.2 Experimental Design and Time Course

Adult C57BI/6J mice were divided into two groups at six weeks old of age and fed with the test diet from 20 weeks. During this experimental period, the ND group (n=23) were fed with a standard diet (4%kcal fat; 5001 from Lab Diet, USA) and the HFD group (n=24) were fed with a high-fat diet (45% kcal fat; D124551 from Research Diets, USA).

The experience was divided in three-time points: 12 (n=17), 16 (n=16) and 20 (n=13) weeks. At the end of each time, the animals were euthanized and pancreas was fixed in 10% neutral-buffered formalin, dehydrated and paraffin-embedded for histological and immunohistochemistry studies.

For this particular study, we focused on 6 animals from the ND group (3 females and 3 males) and 6 from the HFD one (3 females and 3 males), that were randomly chosen. The results were evaluated for week 12 (5 months-old mice), week 16 (6 months-old mice) and week 20 (7 months-old mice).

2.3 Glucose and lipid profile quantification

Blood glucose levels, triglycerides, and low-density lipoproteins (LDL) were quantified weekly in the Central Lab of the Clinical Pathological Department of the Central University Hospital S. João, Porto, using conventional methods with the equipment of the automatic chemistry analysis, Olympus AU5400 (Beckam-Coulter, Izasa, Porto, Portugal).

2.4 Tissues processing for histological techniques labelled

Pancreas from mice on a standard diet or high-fat diet at weeks 12, 16, and 20 were fixed in 10% buffered formalin overnight, then dehydrated with increasing concentrations of ethanol (70%, 90%, and 100%) and diaphanized using 97% xylol. Finally, tissue was embedded in paraffin and 5 μm thick sequential slides were cut and mounted on poly-L-lysine coated slides (1section/slide) and dried for 48 hours at 37 ºC. The slides were used to perform histological stainings and immunohistochemical procedures.

2.5 Pancreas histochemical analysis

2.5.1 Morphological analysis

The morphological evaluation was performed through hematoxylin & eosin (H&E) staining, according to the protocol 1.

The H&E is the standard staining protocol used for light microscope examination of paraffin-embedded tissues. Hematoxylin has no staining properties until it has been oxidized to hematein and combined with a mordant (most commonly aluminium alum). It is a positively charged basic dye, while eosin is a negatively charged acid due. Most cellular organelles and extracellular matrix are eosinophilic (staining positive for eosin, pink colour), while the nucleus, rough endoplasmic reticulum, and ribosomes are basophilic (staining positive for hematoxylin, blue colour). Stain intensity may vary with tissues and fixative solutions.

Protocol 1 – H&E staining

1. Slides were deparaffinized in xylol, during 15 minutes and hydrated with decreasing concentrations of ethanol (100%, 90% and 70%) and lastly rinsed in distilled water for 20 minutes.

2. Slides were stained with Harris Hematoxylin for 10 minutes and rinsed in tap water

3. Slides were rinsed in 90% ethanol and stained with alcoholic eosin at 1% for 2 minutes.

4. Tissues were dehydrated with increasing concentrations of ethanol followed by two xylol passages.

5. Slides were then mounted in Entellan® and air-dried.

6. Pancreas morphology was observed under Nikon Eclipse 501 optical microscope (Amplification: 40x, 100x and 200x) equipped with a digital camera which allowed the capture of representative images at the pancreas-mid section, used for acini and islets morphological evaluation, the measure of islets size, and number.

In H&E stained pancreatic sections, both exocrine and endocrine pancreases were assessed. Acini were evaluated according to the appearance of lining cells, its pyramidal structure, regular patency of the acinar lumen, presence or absence of inflammatory cells, and pyknotic nuclei. Also, ductal changes in the form of epithelial alterations and cellular infiltration were investigated. The islets of Langerhans were evaluated by the presence or absence of intra-islet hemorrhages, vacuolations, nuclear pyknosis, and cellular infiltrates.

The evaluation of the H&E stained pancreatic sections was acceded with the help of Doctor Joana Gomes, Doctor at the Central University Hospital S. João, Porto,

2.5.1.1 Islets size measurement

Measurements of pancreatic islets size were performed via ImageJ[63] program (ImageJ software 1.8.0, Bethesda, Maryland, USA). The diameters of the pancreatic islets were measured in five pancreatic islets/animal, chosen randomly. The presented results provide the mean number of the islets size/animal per section area (μm^2).

2.5.1.2 Islets counting

The total number of islets/sections was determined manually by microscope inspection of each pancreatic section. Five representative pictures were taken. ImageJ[63] program (ImageJ software 1.8.0, Bethesda, Maryland, USA). was used to measure the mean section area (μm^2) of the pancreas in all H&E stained sections. These results provide the mean number of islets number/section area.

2.5.2 Glycogen deposits evaluation

Periodic-acid-Schiff (PAS) staining was performed to quantify the glycogen deposits accumulation in the pancreas, according to protocol 2. PAS staining does not stain only for glycogen, but also other glycoproteins, glycolipids, and some unsaturated lipids and phospholipids. The glycogen is revealed by the Schiff reagent (fuchsin-sulphurous acid), which produces a reddish-purple stain and shows a fibre type pattern. These details can be observed under a light microscope.

Protocol 2 – PAS staining

1. Slides were deparaffinized and hydrated as previously described.

2. Subsequently, they were oxidized in 5% periodic acid solution for 15 minutes, and rinsed, first, in tap water for 5 minutes and then, in distilled water 3 times.

3. Then, tissues were placed in Schiff reagent for 30 minutes and washed in tap water for 5 minutes.

4. Slides were counterstained with Harris hematoxylin for 5 seconds and, again, washed in tap water for 5 minutes.

5. Slides were dehydrated and mounted in Entellan® and air-dried.

6. PAS staining was observed under Nikon Eclipse 501 optical microscope (Amplification: 100x and 400x) equipped with a digital camera which allowed the capture of representative images at the pancreas-mid section, used for glycogen deposits quantification.

2.5.2.1 Glycogen quantification

Pink stain (glycogen) was quantified using CellProfiler program[64] (Cell profiler software 4.2.1, Cambridge, Massachusetts, USA). The program instructions for the histological quantifications are described in the supporting information section (S1).

Four pictures of every animals' pancreas were taken and examined. The results are presented in percentage and provide the mean of the threshold values per total area of the section.

2.5.3 Ca^{2+} deposits evaluation

Von Kossa staining (Protocol 3) was used to assess the deposits of calcium (Ca^{2+}) in pancreas. This technique is used to highlight deposits of Ca^{2+} or Ca^{2+} salt, however, is not specific for the Ca^{2+} ion itself. In this histological method, tissues are incubated in a silver nitrate solution under ultraviolet (UV) light. Deposited Ca^{2+} is reduced by the UV light and the silver deposits will replace the calcium ones. Ca^{2+} salts will be stained in black.

Protocol 3 – Von Kossa staining

1. Slides were deparaffinized and hydrated as previously described.

2. Subsequently, they were incubated with 1% silver nitrate solution in a clear jar (rinsed 3 times in distilled water) placed under UV light for 60 minutes, and rinsed 3 times in distilled water.

3. Slides were incubated with 5% sodium thiosulfate for 5 minutes, to remove the un-reacted silver and, again, rinsed 3 times in distilled water.

4. Slides were counterstained with a fast-red solution for 5 minutes and, once again, washed 3 times in distilled water.

5. Slides were dehydrated and mounted in Entellan® and air-dried.

6. Van Kossa staining was observed under Nikon Eclipse 501 optical microscope (Amplification: 100x and 400x) equipped with a digital camera which allowed the capture of representative images at the pancreas-mid section, used for calcium deposits quantification**.**

2.5.4 Lipofuscin detection

Sudan-Black-B (SBB) histochemical staining was used for lipofuscin examination. SBB stain specifically reacts against lipofuscin, a nonsoluble and nondegradable aggregate of oxidized and cross-linked proteins, lipids, and transition metals that accumulate in non-dividing cells, mainly in the lysosomes.

LB are considered a "hallmark" of aging, once they were described to be accumulated in senescent cells of aged tissues[29,30]. Thus, SBB staining is more often used as a complementary approach with SA- β-gal evaluation for senescence[31].

The positive-SBB stained cells reveal blue-black intracellular granules under the light microscope.

Protocol 4 – SBB staining

1. The pancreatic sections were dewaxed twice with xylol, in a total of 15 minutes, and hydrated with decreasing concentrations of ethanol, from 100% to 70%.
2. Then, slides were stained with Sudan Black 0,1% for 20 minutes and quickly passed through ethanol at 70%, and rinsed in PBS.
3. Finally, slides were mounted in phosphate-buffered glycerol and observed under Nikon Eclipse 501 optical microscope (Amplification: 40x, 100x and 400x) equipped with a digital camera.

2.5.5 Fibrosis quantification

Masson Trichrome (MT) staining and Sirius Red (SR) (or picrosirius red) histochemical techniques were performed for quantification of tissue fibrosis, according to the protocols 5 and 6, respectively. These histological techniques associated with morphometric image analysis allow for qualitative and quantitative characterization of collagen network alterations.

MT is a classical method to visualize connective tissues, particularly collagen, in tissue sections. It reveals the extracellular matrix and highlights the amount and distribution of fibrosis. In the modified version of this staining, collagen fibres are presented in green, due to the light-green dye, the nucleus will be stained for brownish blue/ black and the cytoplasm of the pancreatic cells will be red. This staining is known to yield good results for morphological studies because the different parts of the tissues are very well contrasted.

SR staining provides highly detailed and contrasted staining of connective tissue. It is the optical staining for the evolution of mild or perisinusoidal fibrosis. Due to its high contrast, Sirius red is recommended for morphometric assessment of fibrosis in paraffin-embedded tissue sections. The method is a variant of Van Gieson's staining, which provides red coloration of collagen, but not of the thinnest (reticular) fibres and basement membranes. However, all these structures are stained by SR. In the bright field, collagen appears as bundles of pink to red fibres.

Protocol 5 – Modified MT staining

1. Slides were deparaffinized and hydrated as previously described.

2. Subsequently, incubated with Celestin blue solution for 5 minutes, followed by staining with Gil hematoxylin for 3 minutes

3. Next, slides were differentiated with 1% acid alcohol for 5 minutes and washed with tap water.

4. Ponceau Fuchsin was used for 15 minutes of incubation.

5. Slides were, rinsed in distilled water and treated with 5 % phosphomolybdic acid solution for 10 minutes, and rinsed, again, in distilled water.

6. Finally, slides were incubated with light-green for 10 minutes, rinsed in distilled water, and treated with 1% acetic acid for 2 minutes.

7. Slides were dehydrated and mounted in Entellan® and air-dried for further visualization and analysis.

8. MT staining was observed under Nikon Eclipse 501 optical microscope (Amplification: 100x and 400x) equipped with a digital camera which allowed the capture of representative images at the pancreas-mid section, used for glycogen deposits quantification.

2.5.5.1 Fibrosis quantification with MT staining

Green stain (collagen fibres) was quantified using Cell Profiler programe[64] (Cell profiler software 4.2.1,Cambridge, Massachusetts, USA). The program instructions for the histological quantifications are described in the supporting information section (S1).

The following procedure and the presentation of results are the same described previously for the glycogen quantification.

Protocol 6 – SR staining

1. Pancreas sections were dewaxed and hydrated as previously described.

2. Slides were stained with Red-Sirius solution for 90 minutes, quickly passed through 0.5% acidified water, and subsequently dehydrated with ethanol at 100%, followed by two xylol passages.

3. Slides were then mounted in Entellan® for further visualization and analysis.

2.5.5.2 Fibrosis quantification with SR staining

Red stain (collagen fibres) was quantified using Cell Profiler programe[64] (Cell profiler software 4.2.1,Cambridge, Massachusetts, USA). The program instructions for the histological quantifications are described in the supporting information section (S1).

The following procedure and the presentation of results are the same described previously for the glycogen quantification.

2.6 Amyloid analysis

Congo Red staining is commonly used for the detection of amyloid on paraffin-embedded tissues with amyloidosis.

Amyloid is an amorphous eosinophilic material composed primarily of fibrillar proteins. Deposits of amyloid occur in various organs as a consequence of chronic inflammatory diseases.

There is evidence pointing to the fact that Congo red dye molecules bind to the linearly arranges amyloid fibrils through hydrogen bonds[31].

Positive staining with Congo Red method and the resultant apple-green birefringence with cross-polarization is generally considered the most specific method available to the light microscope for the detection of amyloid.

For the paraffin-embedding tissues, the section specimens should be 6–10 microns. In sections less than 6 microns, amyloid fails to demonstrate birefringence.

Protocol 7 – Congo Red staining

1. Slides were deparaffinized and hydrated as previously described.

2. Subsequently, were incubated in Harris hematoxylin for 2 minutes and washed in tap water for 5 minutes.

3. Slides were washed in distilled water and rinsed in 80% alcohol.

4. Working sodium chloride solution were allowed to react for 20 minutes.

5. Slides were placed directly into the working Congo red solution for 60 minutes.

6. Finally, slides were dehydrated in 3 baths of 100% alcohol and xylol, and then, mounted in Entellan® and air-dried for further visualization and analysis.

2.6 Immunohistochemistry analysis

Immunohistochemical (IHC) techniques were used to evaluate insulin expression in β-cells, using the insulin antibody (INS05 2D11-H5, cat. no. sc833, Santa Cruz Biotechnology, USA); to detect senescent cells in the total pancreas, using the GLB1 antibody (Anti-GLB1/Beta-galactosidase, cat. no. ab203749, Abcam, UK), and to analyse the proliferative state of the pancreas, using PCNA [PCNA (D3H8P) XP® Rabbit mAb, cat.no. #13110, Cell Signalling Technology, USA].

All the immunohistochemical analyses were performed based on protocol 8.

Protocol 8 – IHC labeling

The pancreas sections were deparaffinized and hydrated as previously described.

Antigen retrieval

1. Slides were incubated with citrate buffer 10 mM, 0.05% Tween-20 (pH=6) at 70ºC for 20 minutes

2. After cooling down, slides were washed 3 times with 0.1% PBS Tween-20 (PBS-T), for 5 minutes each time.

Endogenous peroxidase blockade

1. To block any endogenous peroxidase, slides were immersed in a hydrogen peroxide solution at 10% and stored in a humid chamber for 30 minutes.

2. Subsequently, slides were washed in a 1%PBS Triton X-100 solution, for 3 minutes, to occur the permeabilization of the nuclear membrane.

Protein blockade

Background staining was blocked with blocking solution [10% bovine serum albumin (BSA) in 0.1% PBS-T] for 1 hour, at room temperature.

Primary Antibody incubation

Slides were incubated with primary antibodies diluted in blocking solution overnight, at 4ºC, in a wet chamber. Used primary antibodies are presented in Table 1, as well as the concentrations used of each one.

Marked Secondary Antibody incubation

1. Slides were washed in 0.1% PBS-T 2% BSA solution
2. Then, they were incubated with the secondary antibody diluted in blocking solution for 1h in a wet chamber, at room temperature. The secondary antibodies used in this step are presented in Table 2, as well as their respective concentrations.

Avidin-Biotin Complex

1. After that, slides were washed carefully with a 0.1% PBS Triton X-100 solution, 3 times, 5 minutes each time.
2. ABC (avidin-biotin complex – Vector Laboratories) (1:200) was then added to the slides and incubated for 30 minutes, at room temperature.
3. Slides were washed, again, with a 0.1% PBS Triton X-100 solution, 3 times, 5 minutes each time.

Stain and counterstain

1. DAB (3, -3'diaminobenzidine) solution (2,5 mg DAB in 0,05M Tris-HCl in H_2O) was added to the slides, for 15 seconds, to reveal the stain and quickly washed in PBS 1% for 5 minutes.
2. Counterstaining was performed next by immersing the slides for 1 minute in Harris hematoxylin.
3. Finally, slides were dehydrated and mounted in Entellan® and air-dried for further visualization and analysis.

Table 1
Primary antibodies (IHC)

Antibody	Mark	Reference	Host species	Concentration
Insulin (AD11-H5)	Santa Cruz Biotech	Sc-8033	Mouse	1:100
GLB1/Beta-galactosidase	Abcam	ab203749	Rabbit	1:200
PCNA (D3H80)	Cell Signalling	#13110	Rabbit	1:200

Table 2
Secondary antibodies (IHC)

Antibody	Mark	Reference	Conjugate	Concentration
mouse anti-rabbit IgG-B	Santa Cruz Biotech	Sc-2491	Biotin	1:1000
m-IgG$_k$ BP-B	Santa Cruz Biotech	Sc-516142	Biotin	1:900

2.6.1 Insulin expression quantification

Antibodies against insulin are widely used in the pancreas to evaluate the β-cells insulin production. The results of this evaluation are usually combined with the results of the glycaemic levels, to inform about the metabolic state of pancreatic β-cells.

Insulin expression was quantified using Cellprofiler program[65] (Cell profiler software 4.2.1, Cambridge, Massachusetts, USA). The program instructions for the immunohistochemistry quantifications are very similar to the ones for the histological quantifications, which are described in the supporting information section (S1).

The following procedure and the presentation of results are the same described previously for the glycogen quantification.

Also, it was performed a categorical method to analyse the immunostaining intensity of pancreatic islets' insulin. The used scale goes from 0 to 3+, where 0 means no pancreatic islets stained, 1+ means pancreatic islets with low stain, 2+ means pancreatic islets with high stain and 3+ means pancreatic islets very high stained.

2.6.2 Pancreatic senescent content quantification

The activation of the *GLB1* gene was discovered to be the source of the SA-β-gal activity, and its expression correlates with SA-β-gal activity both *in vitro* and *in vivo*[66].

Specific markers of senescence have been lacking, especially those that can work in paraffin-embedded tissues. So, the specificity of the GLB1 antibody directed against the lysosomal portion of SA-β-gal was confirmed before in cellular models of replicative senescence in ones using mice and human tissues[25,67].

Senescent cells content was quantified using Cellprofiler program[65] (Cell profiler software 4.2.1, Cambridge, Massachusetts, USA). The program instructions for the immunohistochemistry quantifications are very similar to the ones for the histological quantifications, which are described in the supporting information section (S1). The following procedure and the presentation of results are the same described previously for the glycogen quantification.

2.6.3 Proliferative cells quantification

Proliferating cell nuclear antigen (PCNA) is a nuclear nonhistone protein that is considered essential for DNA synthesis and that is described as an accessory protein for DNA α-polymerase (present during G1/S phase of the cell cycle). So PCNA is expressed mainly in late G1 and S and is a commonly used general cell proliferation marker.

Proliferative cells content was quantified using Cellprofiler program[65] (Cell profiler software 4.2.1, Cambridge, Massachusetts, USA). The program instructions for the immunohistochemistry quantifications are very similar to the ones for the The following procedure and the presentation of results are the same described previously for the glycogen quantification.

2.7 Statistical analysis

To evaluate the statistical differences between groups, two-way ANOVA followed by Sidak multiple comparisons and chi-square tests were performed. Two-way ANOVA followed by Sidak multiple comparisons test was used to determine statistical significance for food consumption, weight, glycaemic, lipidic, islets area, insulin expression, glycogen accumulation, collagen deposition and, GLB1 and PCNA stained cells results. Chi-square test was used to evaluate the statistical significance for islets number and insulin expression intensity.

For the quantification analysis, a minimum of four and a maximum of five photos were taken randomly to each slide. Then, all images were quantified and the final result is presented by the mean of the results for each animal pancreatic section. Data were presented as mean ± standard error of the mean (SEM) and p-value <0.05 was considered statistically significant. The statistical analyses were performed using GraphPad Prism 8.0.1 (GraphPad Software, San Diego, CA, USA).

3. Results and Discussion

3.1 Evaluation of the nutritional data and biochemistry parameters

3.1.1 Food consumption

The energy intake by the animals was monitored weekly during the time of study (*Figure 5*). It was verified that the ND group ingested in average 85,74± 6.28 g/week, while the HFD group only ingested 72,20±8.99 g/week (*Figure 5A*), with significant results between the two groups at week 4 and 6.

These results are supported by the fact that the HFD animals have an increased caloric intake per diet what rendering them more satisfied with less amount of food. So, we perceived that the food consumption reduction observed in the HFD group is inversely correlated with the caloric composition of the diet.

An analysis of food intake by gender (*Figure 5B*) revealed that males ingest more ration than females, without significant differences.

In the ND group, the averages of food intake for the males (85.20±6.43 g/week) and females (84.29±7.19 g/week) didn't present significant differences opposing to the HFD group, where males (79.58±19.59 g/week) revealed an increase comparing to females (66.16±11.80 g/week). It is known that males require higher amounts of energy source comparing to females and that's one of the reasons why, in the current study, males are characterized by increased body weight (*Figure 6)* and increased glucose levels (*Figure 7*)[68].

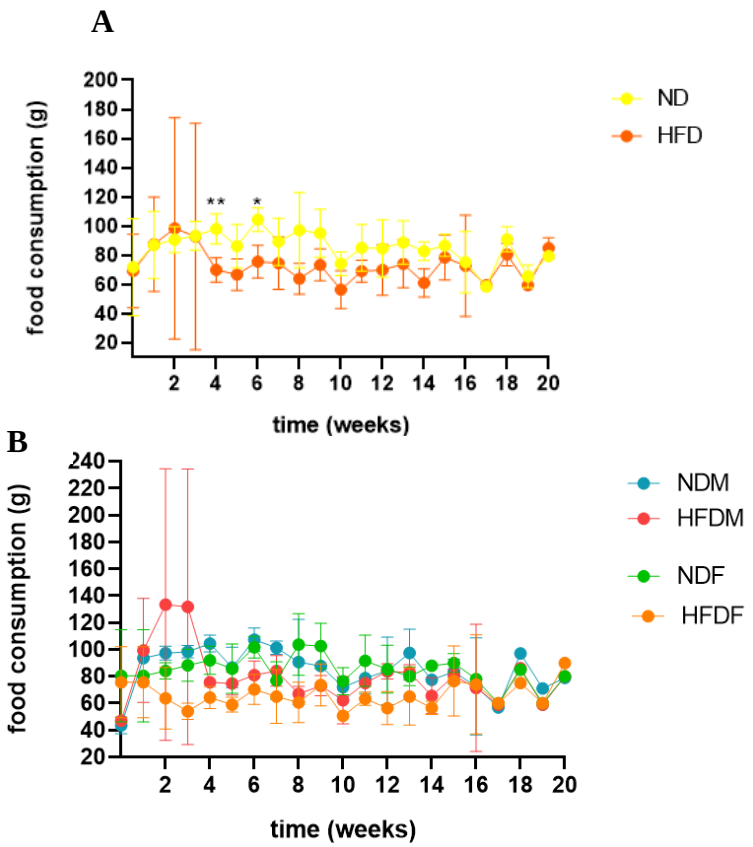

Figure 5. Representative curves for food consumption by C57BL/6J mice, monitored over 20 weeks. A- The average of food intake results per week from every animal present in the study for normal diet (ND) animals comparing to hight-fat diet (HFD). B-The food intake by gender for normal diet female (NDF) (n=3), hight-fat diet female (HFDF) (n=3), for normal diet male (NDM) (n=3), and hight-fat diet male (HFDM) (n=3). A- *P<0.05, **P<0.01. Results are expressed in average ± SEM. P values were determined by the two-way ANOVA test, followed by the Sidak test.

3.1.2 Weight

Figure 6 represents the curves for the body weight changes according to age (in weeks). Up to 10th week, the weight for the two experimental groups was very similar, with the ND group weighted, on average, 22.17±0.60 g and the HFD group with 22.41±0.89 g. Over the 20 weeks, both groups increased their weight levels, with the HFD animals (37.33± 4.49g) reaching superior values compared to the ND (29.50± 2.41g) (*Figure 6A*). These results are supported by previous studies where is described an increase in body weight of the adult C57BL/6 mice fed by an HFD, compared to the control group, right after 9 weeks of study. [69,70]

Comparing the weight values between males and females from the ND and HFD groups, we observe significant differences, right from the first week (*Figure 6*B).

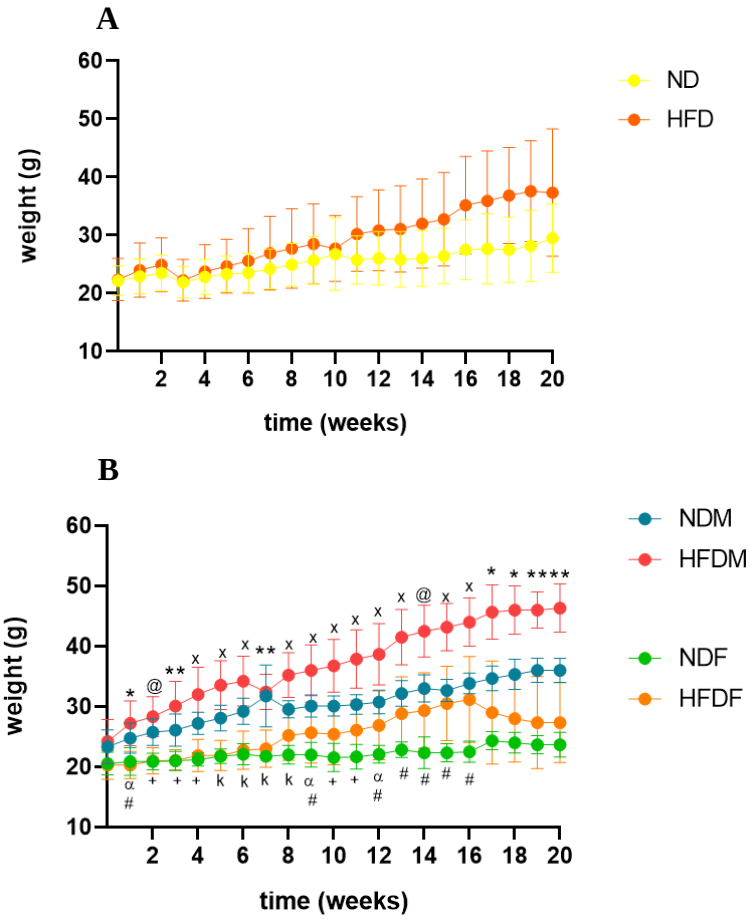

Figure 6. Representative curves for bodyweight variations of C57BL/6J mice, monitored over 20 weeks. A- Bodyweight curves for the normal diet (ND) group and hight-fat diet (HFD) group, over 20 weeks. B- The body changes by gender for normal diet female (NDF) (n=3), hight-fat diet female (HFDF) (n=3), normal diet male (NDM) (n=3) and hight-fat diet male (HFDM) (n=3). B-**P*<0.05, ***P*<0.01, @ *P*<0.001, x *P*<0.0001; when compared with the values for the HFDF, and #*P*<0.05, α#*P*<0.01, +*P*<0.001, k*P*<0.0001; when compared with the values for the NDM. Results are expressed in average ± SEM. P values were determined by the two-way ANOVA test, followed by the Sidak test.

3.1.3 Glycaemia

The first biochemistry parameter to be analysed was the glucose levels. They were monitored over 20 weeks in each animal (*Figure 7*). In week 0, ND and HFD mice presented normal glycaemic levels.

In *Figure 7A*, we observe that the glycaemia levels for the HFD group were predominantly superior from ND, although it only reached statistical significance at week 11. At week 20, both ND and HFD groups had a decrease in their glucose levels. The average glucose levels for the ND animals was 158.17±7.36 mg/dl and for the HFD ones was on average 162.17±6.30mg/dl.

In this study, the animals with a control diet had a lot of variations in their glucose levels over time, with an unpredictable decrease at week 20. But even at that timepoint, the values were still elevated. Previous studies demonstrate that, in animals fed with a low lipidic content diet, the glucose levels ranging between 100 mg/dl and 130 mg/dl in C57BL/6J mice over several weeks, although these values could increase in older animals[71,72,73].

Glucose levels were also analysed by gender. The range of glycaemic values for healthy individuals is around 175 mg/dl for females and 200 mg/dl for males. Likewise, the glucose levels for the males were predominantly superior to the females, as for the ones with an ND and with an HFD (*Figure 7B*). At week 12, we observe that the levels of the HFDF (177±8.04 mg/dl) and HFDM (200.44±6.03 mg/dl) are superior comparing to the ones for NDF (133.22 ±11.29 mg/dl) and NDM (176.11±9.17 mg/dl). At week 16, both HFDF and HFDM continued to demonstrate high glucose levels (221.50±31.07 g/dl for the females and 201.500±7.77 g/dl for the males), and, finally at week 20, there was a decrease in glycaemia levels for all 4 groups and the levels became similar.

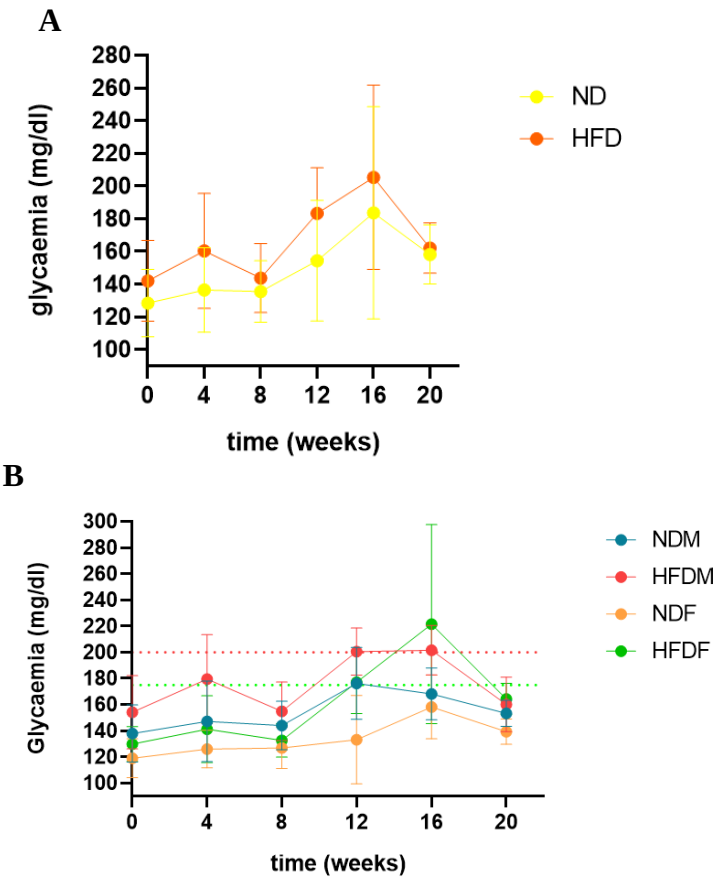

Figure 7. Representative curves for the glucose levels of C57BL/6J mice, monitored over 20 weeks. A- Glucose levels for the normal diet (ND) group and high fat diet (HFD) group, with a significant increase in HFD glycaemic levels at week 11, comparing to the ones for the ND group. B- Glucose levels by gender for normal diet female (NDF), hight-fat diet female (HFDF), normal diet male (NDM) and hight-fat diet male (HFDM). Streak green and pink lines represent the standard value of glycaemia for healthy female and male mice, respectively. Results are expressed in average ± SEM. P values were determined by the two-way ANOVA test, followed by the Sidak test.

Henceforward, since we do not obtain significant differences between males and females, we decided to present the remaining results just for the ND and the HFD animals, without gender evaluation.

3.1.4 Lipid profile

The levels of the total cholesterol and levels of the lipoprotein LDL were measured over the time of the study.

Cholesterol levels show a significant difference between the total levels for the ND animals and the HFD, with the HDF showing superior levels every week comparing to the ND (*Figure 8A*). Regarding the plasmatic LDL levels, in *Figure 8B* it is demonstrated that occurs an increase in the concentration of these low-density lipoproteins in the HFD group compared to the ND ones, with very significant differences at the weeks 16 and 20 weeks.

The increasingly cholesterol and LDL levels observed in HFD mice are also described for obese mice and human patients[74,53].

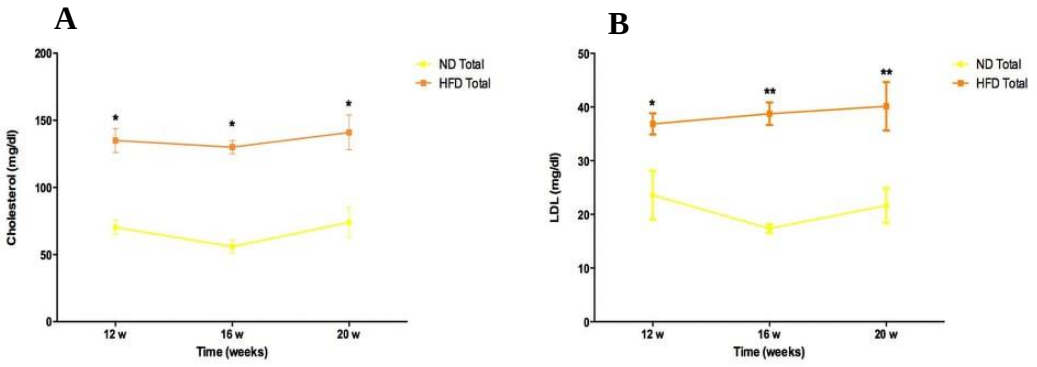

Figure 8. Representative curves for the total cholesterol and the plasmatic concentration of LDL of C57BL/6J mice, monitored over 20 weeks**.** A- Total cholesterol levels for the normal diet (ND) group and high-fat diet (HFD) group, with significant results for HFD animals at weeks 12, 16, and 20, compared to ND ones. B- Plasmatic concentration of the LDL for the normal diet (ND) group and high-fat diet (HFD) group, with a significative increase in the values for HFD animals with age, in weeks, compared to ND ones. A-**P*<0.05. B-**P*<0.05, ***P*<0.01. Results are expressed in average ± SEM. P values were determined by the two-way ANOVA test, followed by the Sidak test.

Many studies suggests that type-2-diabetes (T2D) can be induced in this experimental model by the ingestion of a diet with high caloric intake[69,72].

In this experimental study HFD animals present increased weigh levels, high plasmatic glucose levels and increased lipidic parameters, which means that these animals were certainly obese. However, they do not reach the diabetic state since we do not observe sustain glycaemic levels after week 16 (which means that the animals are not insulin resistances). In contrast, we observe a reversion of the high glycaemic levels between week 16 and 20.

3.2 Morphological evaluation

3.2.1 Histopathology

Histology of the ND and HFD mice pancreas was analysed by an H&E staining.

For the ND animals at week 12, the islets of Langerhans are regular and well-defined. They present pale stain areas, surrounded by deeply stained peripherally located pancreatic acini. The endocrine cells of the islets appeared with pale acidophilic cytoplasm and central vesicular nuclei. The exocrine pancreas showed normal histology structure in the form of regular, closed packed, patent acini lined by pyramidal cells (*Figure 9A*). With age, at weeks 16 and 20, we observe an increase in the islets' size and disrupted histoarchitecture of the islets (loss of the normal cellular cord arrangement) and the acini (opening between cells, nuclear pyknosis, vascular changes, and congested blood capillaries) with infiltration of inflammatory cells (probably lymphocytes).

Morphological characteristics are similar between ND and HFD animals in weeks 12 and 16, and, at the age of 7 months (week 20), appears to occur a histopathological recovery of the pancreas morphology. Islets size appears to be very similar to the ones for the ND group at week 12, also islets structure cells appear to be repaired and the exocrine cells back to exhibit normal histology structure, with regular form and closely packed (*Figure 9B*). These results suggest that the pancreas of the aged animals under a HFD can recover from the damages caused by this type of diet over time and present better histology compared to the pancreas of the aged healthy mice.

3.2.2 Islet size

Analysis of the mean area of pancreatic Langerhans islets among the studied groups (*Figure 10*) showed a significant increase in the mean area for ND mice, in week 16 and 20, corroborated by previous studies, where it was concluded that the mean diameter of the islets of Langerhans increase with age in healthy rodents, at least at the age of 1 year old, which is thought to be the limit age in mice for turnover and plasticity islet cells mechanisms[45].

Regarding the HFD group, in week 12 and 16, occurs an increase in the islet area, which is not significant, and then at week 20, the area of the islets significantly decreases comparing to the results at week 16. These results infer that glycaemic levels are positively correlated with the insulin demand, β-cell mass and, consequently the islets size[75]**.**

Comparing the 2 groups, we also can detect significant differences for the mean area of the islets. There is a significant increase of HFD animal's islets, at week 16. Also, at week 20, there is a significant decrease of HFD animal's islets at comparing to the ND values. These results are contradictory with the ones observed for obese mice along age[58], however they are supported by the glycaemia levels presented in this study and the insulin expression results that will be discussed further ahead.

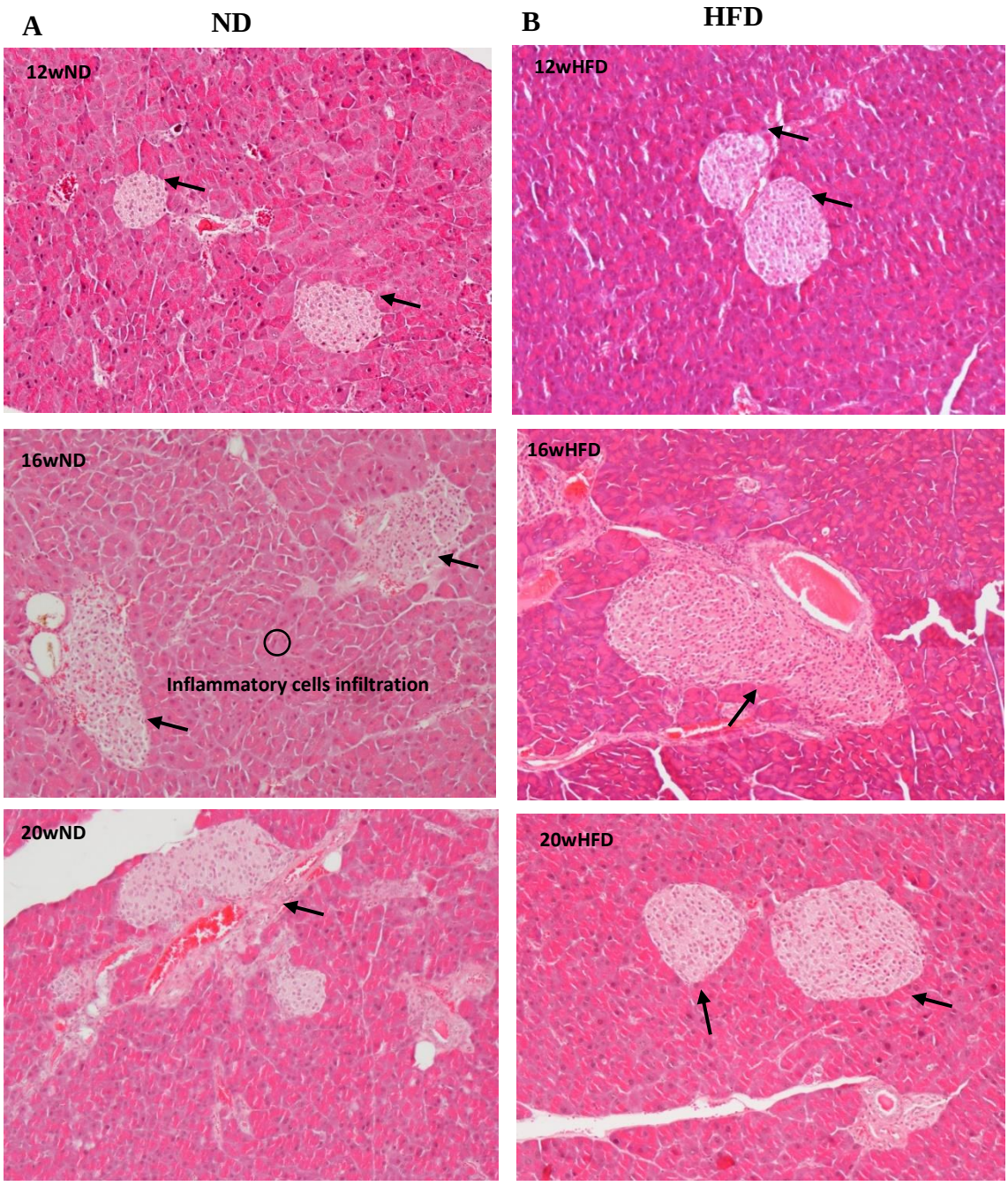

Figure 9. Representative images for the H&E staining at weeks 12, 16, and 20 (Amplification: 100x) for the (A) normal diet (ND) mice pancreas and (B) high-fat diet (HFD) mice pancreas. Arrows pointing for the structure of pancreatic islets. ND mice present normal acini structure and round islets, in week 12. In week 16 and 20, we can observe an increase in the pancreatic islets and its deformation, with a disruption of the acini normal histoarchitecture and inflammatory cells infiltration. For the HFD group, at week 12 we already see deformation in pancreas structure, especially in the morphology of the exocrine pancreas, then at week 16, an enlargement of the islets is noticed, due to an increase in β-cell insulin production, in order to decrease the hyperglycaemic levels. At week 20, it is observed a recovery in pancreas morphology for the HFD animals, suggesting a metabolic change in the pancreas of aged obese mice.

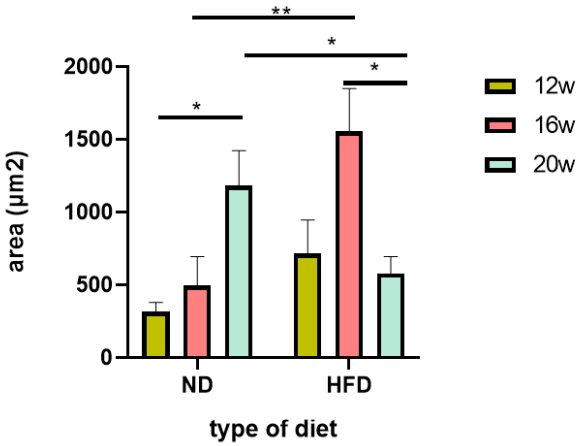

Figure 10. Mean values of the pancreatic Langerhans islets area for mice fed with different diets -normal diet (ND) group and high-fat diet (HFD) group- at weeks 12, 16, and 20. There is a significant increase in the mean area for ND mice, between weeks 16 and 20 and a significant decrease of HFD's mean islets area at week 20. Comparing the ND with the HFD group, there is a significant increase of HFD's mean islets area at week 16 and a significant decrease at week 20. **P*<0.05, ***P*<0.01. P values were determined by the two-way ANOVA test, followed by the Sidak test.

3.2.3 Islets Number

Previous studies suggest that hyperglycaemic levels in humans and rodents are associated with an increased in the islets number by the hyperplasia and/or hypertrophy of islets β-pancreatic cells[76,77,75].

Looking at *Figure 11*, we realize that at week 16, the one where HFD animals reach higher levels of glucose in plasma, there is a notable increase in islets number of the HFD animals. Overall, the results for the islets number follow the ones for the size of the islets.

We could not determine the source for the increased number of islets in obese mice, however, previous studies suggested that new islets can be formed by proliferation by existing differentiated islets cells, undifferentiated stem cells, or maybe by neogenesis from pancreatic ducts[78,79,80].

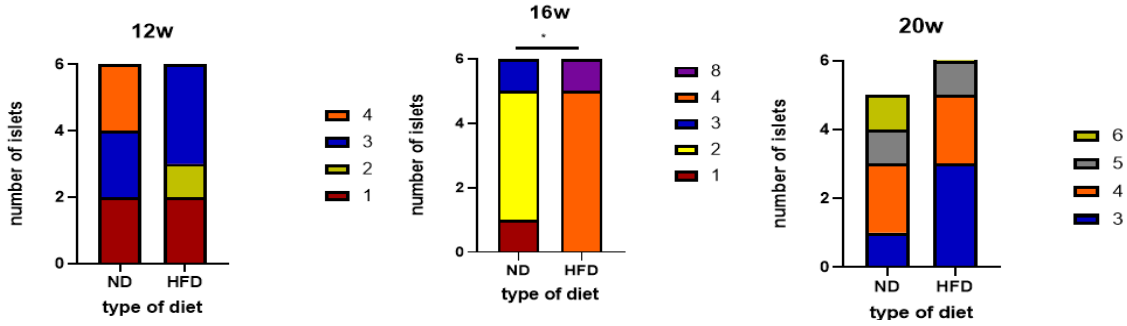

Figure 11. Number of islets in mice pancreas fed with two diets -normal diet (ND) group and high-fat diet (HFD) group- at weeks 12, 16, and 20. At week 16, there is a significant increase in the islets number of the HFD animals. **P*<0.05; when compared with the values for the ND total values. P values were determined by the Chi-square test.

3.3 Insulin Expression

Positive insulin expression is visualized as dark-brown cytoplasmatic granules in the pancreatic islets' β cell (*Figure 12*). The quantitative analysis of insulin expression per area of the pancreatic islets did not show significant variations between both conditions (*Figure 13*).

The results for the ND animals, do not show significant differences for the insulin expression between weeks 12, 16, and 20 (the results present high standard-deviation bars which probably suggest that the n of the animals used at each week was not sufficient to see significant differences in insulin expression between them).

Regarding the HFD individuals, we observe a significant decrease in values for the insulin expression at week 20. These results follow the ones for the islet size and number and, also, the glycaemic levels.

The immunostaining intensity of pancreatic islets' insulin was obtained by a categorical method. The staining intensities of insulin in the pancreatic islets among different study groups are shown in *Figure 14*. For the ND animals, it seems to have a gradual decrease in the intensity of the insulin expression in the islets. This may suggest a decrease in the levels of insulin production in β-cell healthy mice with age.

At week 12, there are no significant differences in the results for the insulin staining intensity between the groups. At week 16, there is a significant increase in insulin staining intensity for the HFD and, at week 20, the HFD animals show the lowest insulin staining intensity.

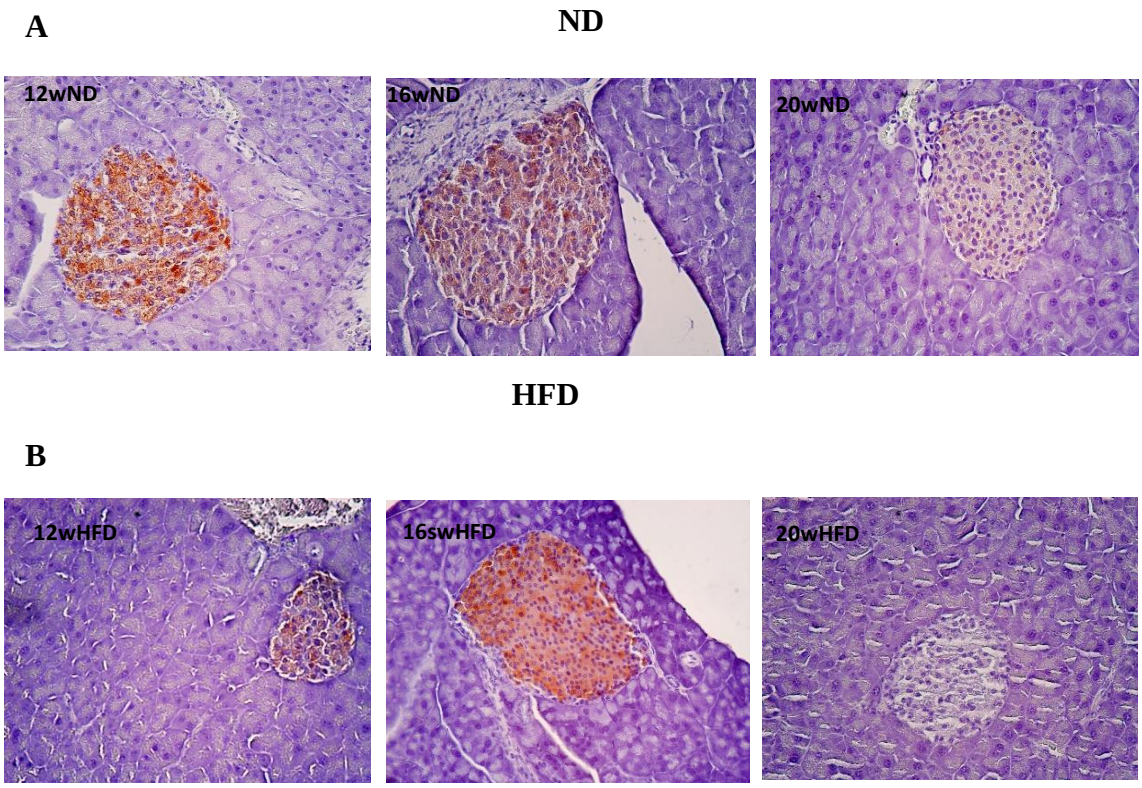

Figure 12. Representative images for the results for insulin expression immunohistochemistry at weeks 12, 16, and 20 (Amplification: 200x) for the (A) normal diet (ND) mice islets and the (B) hight-fat diet (HFD) islets mice. The brown in the cytoplasm of pancreatic islets of Langerhans means that islets cells are staining positive to insulin. For ND animals, it is noticed a gradual decrease in insulin expression and in the intensity of it with age, in weeks. HFD animals have a clear increase in insulin expression at week 16 and then, at week 20, we do not see any stain. The differences for the insulin expression between the two groups are also very visible.

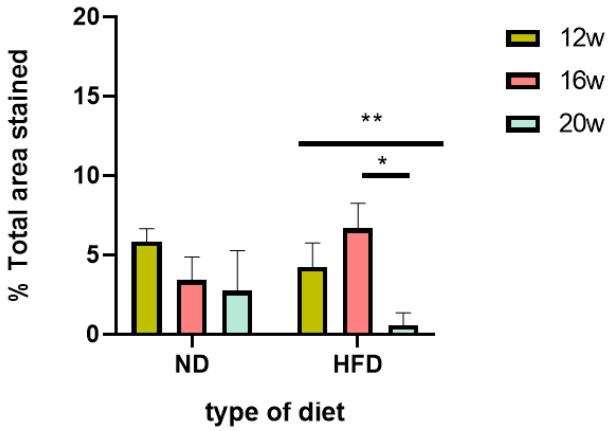

Figure 13. Insulin expression in mice β-pancreatic cells with distinct diets- normal diet (ND) group and high-fat diet (HFD) group- at weeks 12, 16, and 20. No significant differences were demonstrated for the ND group. For the obese group we see a significant decrease in values for insulin expression at week 20, compared to the levels for the weeks 12 and 16. **P*<0.05 and ***P*<0.01. P values were determined by the two-way ANOVA test, followed by the Sidak test.

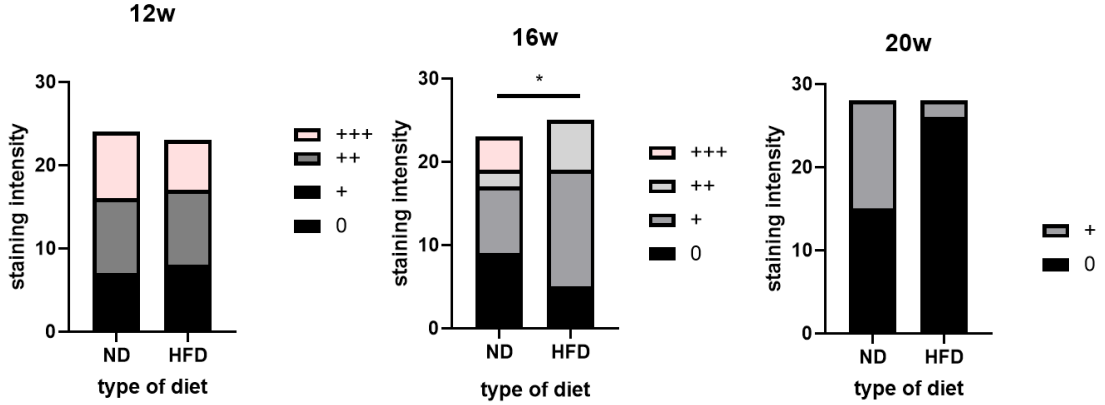

Figure 14. Intensity of the insulin expression in mice β-pancreatic cells for the two different diets- normal diet (ND) group and high-fat diet (HFD) group- at weeks 12, 16, and 20. At week 16, there is a significant increase in insulin staining intensity in the HFD islets cells. Then, at week 20, the HFD animals show the lowest insulin staining intensity. **P*<0.05, ****P*<0.001; when compared with the values for the ND total values. P values were determined by the Chi-square test.

Up until now, we see that the results for islets sizes and number and these that elucidate for insulin production support the data for the glycaemic levels. However, in the obese subjects the decrease in insulin expression at week 20, may also refer to an impairment in the metabolism of pancreatic β-cells. Thus, to clarify this question, the presence of glycogen deposits and the Ca^{2+} deposits were evaluated.

3.4 Glycogen Deposits

PAS staining is often used in the paraffin-embedded sections to evaluate the glycogen deposits.

Glycogen accumulation is associated with an impairment in β-cells metabolism and is often observed in islets of rodents and patients with chronic hyperglycaemia[81].

We performed a qualitative evaluation of the glycogen deposits (*Figure 15*) and a quantitative analysis of the glycogen content (*Figure 16*).

In *Figure 15*, we distinguish the presence of small amounts of glycogen deposits in exocrine and endocrine pancreas of all subjects of the two groups with a decrease in glycogen content in the obese pancreas at week 20, when both exocrine and endocrine pancreas are considered, confirmed by the results of the glycogen quantification (*Figure 16A*).

Regarding the results for the glycogen deposits in the endocrine pancreas (*Figure 16B*), glycogen accumulation in islets is residual for both groups at each time point (very little percentages of glycogen content) and also, no significant differences for both groups are noted with time.

These results suggest that glycogen deposits have not a significant influence in the pancreatic β-cells metabolism in young and adult mice, regardless of the type of diet.

A **ND** **B** **HFD**

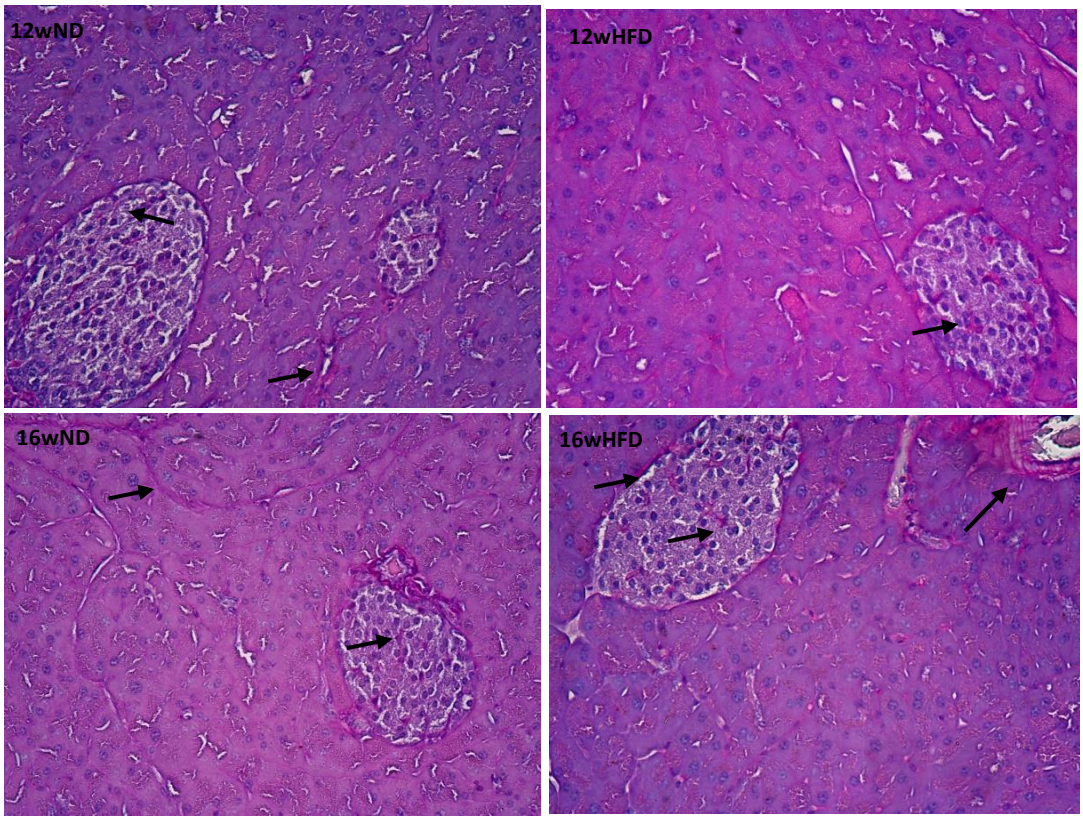

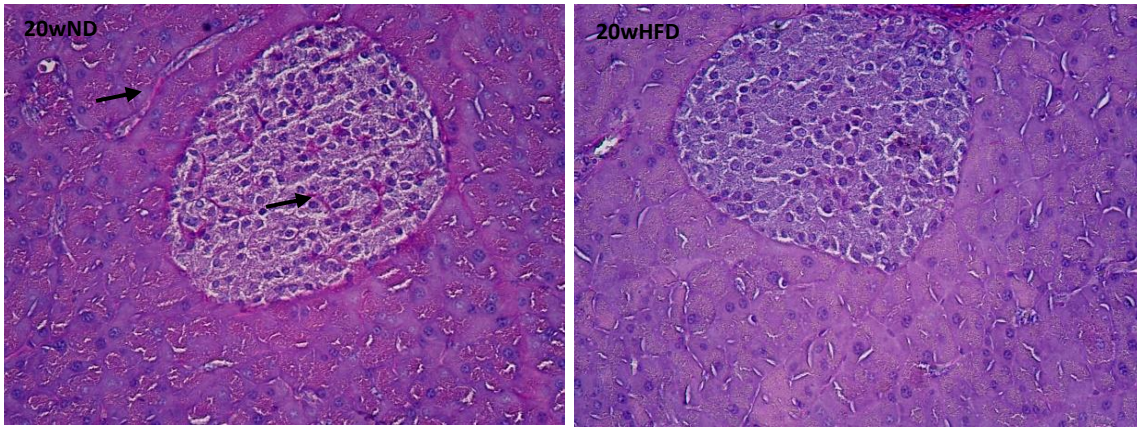

Figure 15. Representative images for the PAS staining results at weeks 12, 16, and 20 (Amplification: 200x) for the pancreas of (A) the normal diet (ND) mice and (B) the high-fat diet (HFD) mice. The pink colour (arrow) around the cells of the pancreatic islets and between acini is staining for glycogen deposits. For ND animals, we do not see any differences in pancreatic glycogen content with age. However, in HFD animals, at week 20, we see a decrease in pink colouration around the islets, around islets cells, and between acini.

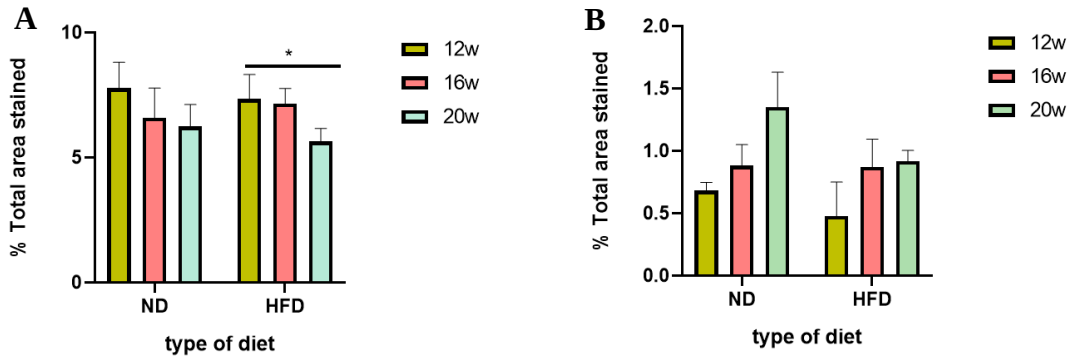

Figure 16. Quantification of pancreatic glycogen accumulation in mice C57BL/6J, for the two diet groups- normal diet (ND) group and high-fat diet (HFD) group- at weeks 12, 16, and 20. A- Results for total pancreas with a significant decrease in the glycogen accumulation in HFD group, at week 20. B- Results for the islets. There are no significant results. **P*<0.05 P values were determined by the two-way ANOVA test, followed by the Sidak test

3.5 Ca^{2+} accumulation

Pancreatic Ca^{2+} deposits accumulation and calcification of pancreatic blood vessels are important characteristics of chronic pancreatitis. Obese individuals have an increased risk of developing this disease, that can be responsible for tissue damage over time and increased prevalence of T2D by disrupting β-cells insulin production[82].

On the other hand, previous studies using aged human pancreas suggested an increase in calcification of the pancreatic blood vessels over time[83].

Here we used the Von Kossa staining to evaluate possible Ca^{2+} deposits accumulation over time in ND and obese subjects.

The results are presented in *Figure 17* and the groups did not presented Ca^{2+} deposits in the pancreas with time. The results for the ND group may be justified by the fact that the animals used for this experimental work were not considered as old, which may suggest that Ca^{2+} depositions are only visible in older animals. Regarding the results for the obese mice, the absence of Ca^{2+} deposits is supported by the results of the insulin expression, which suggested a good function of pancreatic β-cells.

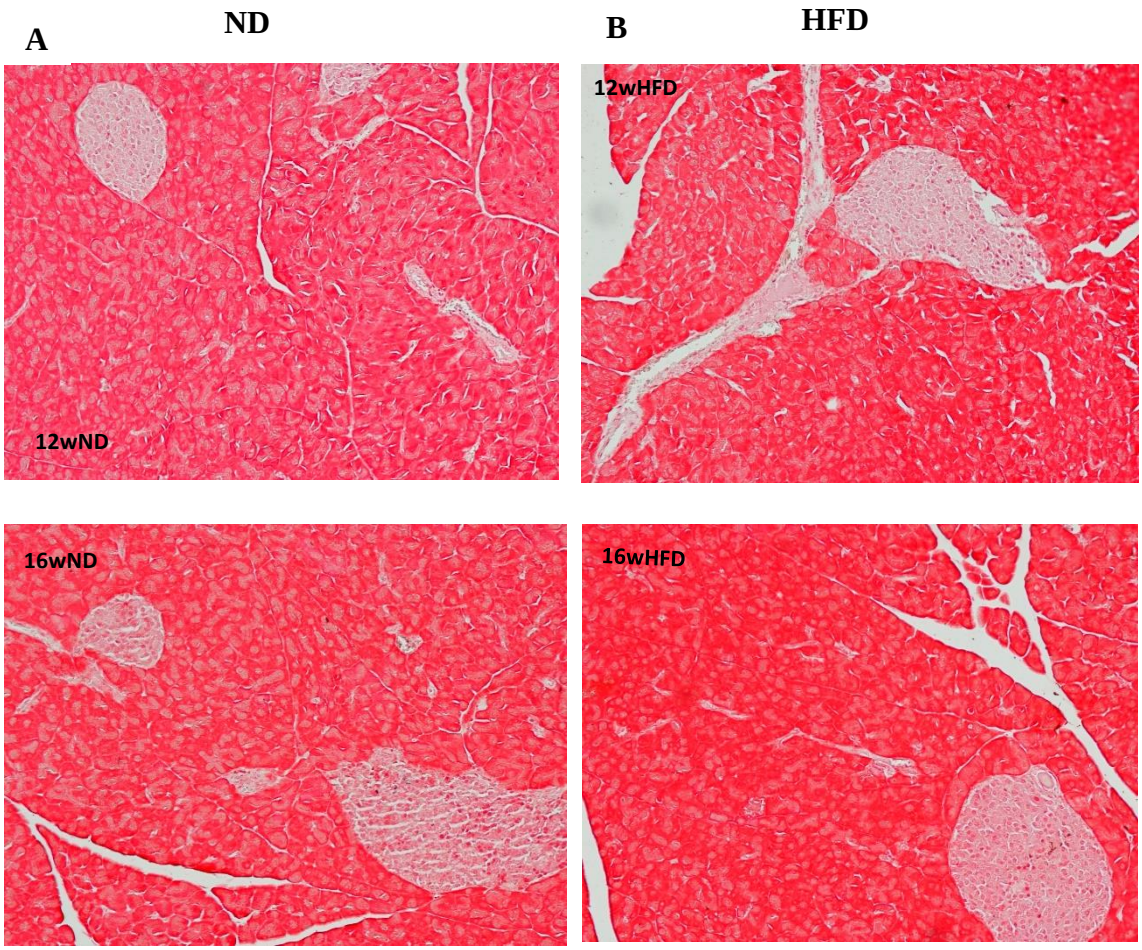

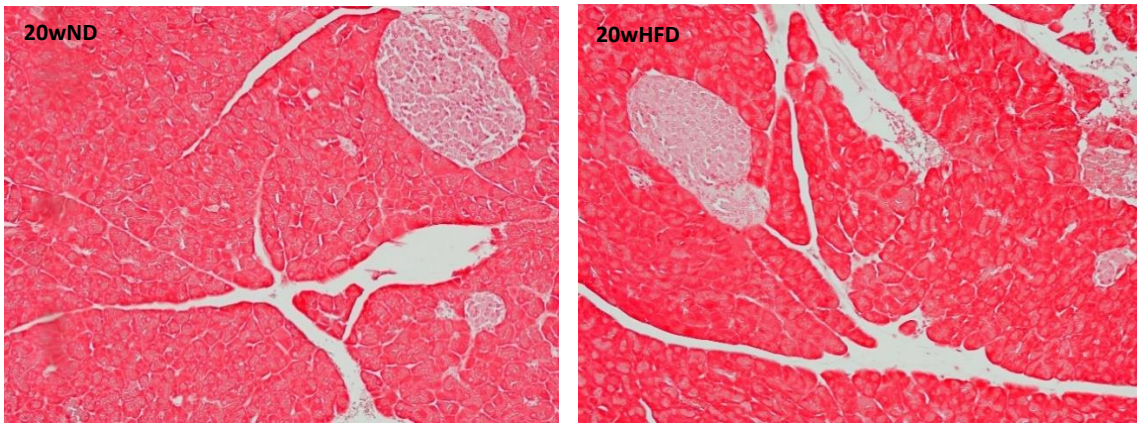

Figure 17. Representative images for the Von Kossa staining results at weeks 12, 16, and 20 (Amplification: 40x) in mice pancreas of the (A) normal diet (ND) and the (B) high-fat diet (HFD) group. There are no ca^{2+} deposits in acini or calcification of pancreatic blood vessels.

3.6 Senescent markers

A limit number of studies have focused on the role of the pancreas cells senescent state. It is known that pancreatic structure and function undergo multiple changes with aging and senescence, which may tend to result in pancreatic diseases as the body ages[45].

Previous studies, conclude that diabetic C57BL/6J mice provoked by a high-fat diet and associated with obesity, hyperglycaemia and hyperinsulinemia will increase β-cell proliferation and the generation of ROS on β-cells, a characteristic of senescent cells[84,85]. Also, there are findings suggesting that β-cell senescence occurs in diet-induced T2D, contributing to the pathogenesis of the disease[60].

Regarding these evidences we intended to evaluate the senescence content in pancreas mice for the ages of 12, 16 and 20 weeks. Although adult animals have been used, we expected to observe an increase senescent content at week 12 and 16 in the obese pancreas. At week 20, since previous studies suggest a pancreatic metabolic recovery for the HFD animals, we were curious to know about the senescent state of obese pancreatic cells.

Senescent cell content was evaluated throw a specific marker for senescent cells, GLB1-antigen, Sudan Black staining, specific for lipofuscin detection and PCNA-antigen, proliferation marker.

3.6.1 GLB1 expression in pancreatic cells

GLB1 antibody was used to detect senescence on pancreatic cells of the animals at weeks 12, 16 ad 20. First, we evaluated the GLB1 expression on the pancreas in general and then we analysed these values just for the endocrine pancreatic cells.

In Figure *18A*, we notice that for the HFD group, at week 12, the senescence content per area on the pancreas was significantly increased. This may be explained by the fact that, at week 12, the HFD animals were already obese and had high levels of glucose in the plasma, which will cause a metabolic impairment and, consequently, an increase in cellular senescence content[86]. At week 16, there is an increase in GLB1 staining comparing to week 12 and then, at week 20, there is a decrease in cells staining positive for GLB1 on the HFD group (noun of these differences was significant).

Then, looking at *Figure 18B*, where is presented the effect of the diet along time in the endocrine pancreas, we see a very similar variation in the content of cells staining positive for GLB1 to the one presented in *Figure 18A*, with a significant increase in the positive stain from week 12 to 20 in the ND group and also a significant decrease in the positive stain between the ND group and the HFD group at week 20.

The immunohistochemistry results are presented in *Figure 18*.

Firstly, these results prove that even in an adult phase, there are already the formation of senescent pancreatic cells, which will increase along time. Also, these results suggest a direct relationship between the total pancreatic cellular senescence and the cell senescence of the endocrine pancreatic cells, with the islet cells being more affected by the cellular senescence process then acini cells. In fact, for ND mice, we observe higher glucose levels that the ones that were expected with a decrease in insulin response with time, which may be explained by an impairment in the β-cells function due to the cellular senescence process[45].

Additionally, the results obtained for the GLB1 staining positive cells in HFD mice suggests that, in obese animals, at adult age, with time, the hyperglycaemic demands may be superior to the β-gal-senescence deleterious effects on islets cells. This idea is supported by previous studies, where it was found that p16-induced senescence of pancreatic β-cells enhances glucose-stimulated insulin secretion and improves glucose tolerance in diabetic mice[62]. Also, the decrease in the β-gal-senescence cell content at week 20, in obese mice, maybe be to a repair in β-cell metabolism (justified by a decrease in insulin production and so the normalization of the glycaemic levels- *Figures 7A* and *13*) or due to an increase in cell proliferation. To evaluate this last possibility, immunohistochemistry for a proliferation marker was performed.

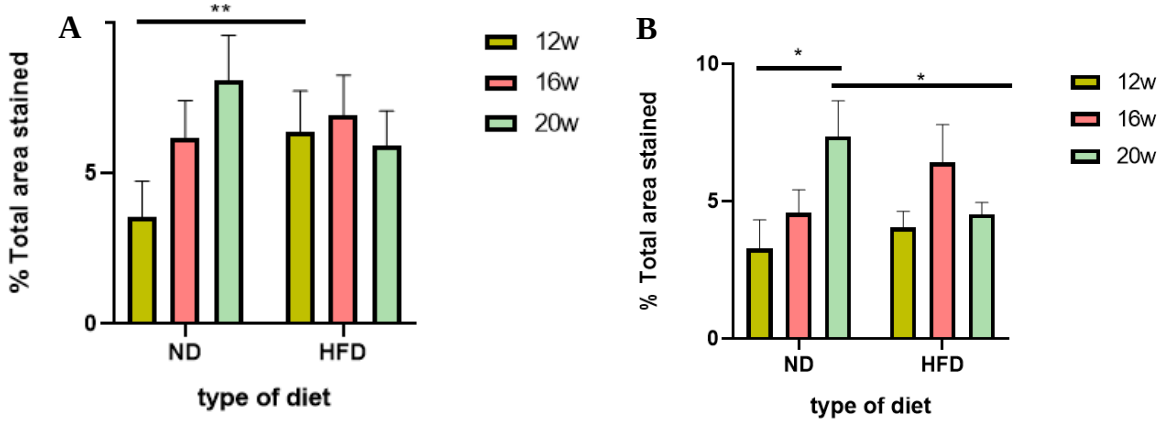

Figure 18. Pancreatic cells staining positive for GLB1 in mice fed with two diets- normal diet (ND) group and high-fat diet (HFD) group- at weeks 12, 16, and 20. A- Results for total pancreas with significant differences between the results for the GLB1 staining positive cells for ND and HFD group, at week 12. B- Results for the islets. Similar to the ones presented at A. There is a significant increase in GLB1 positive cells with time for the ND group and a notable decrease in senescent cells for the HFD group at week 20 when compared to the values for the ND. **P*<0.05 and ***P*<0.01. P values were determined by the two-way ANOVA test, followed by the Sidak test.

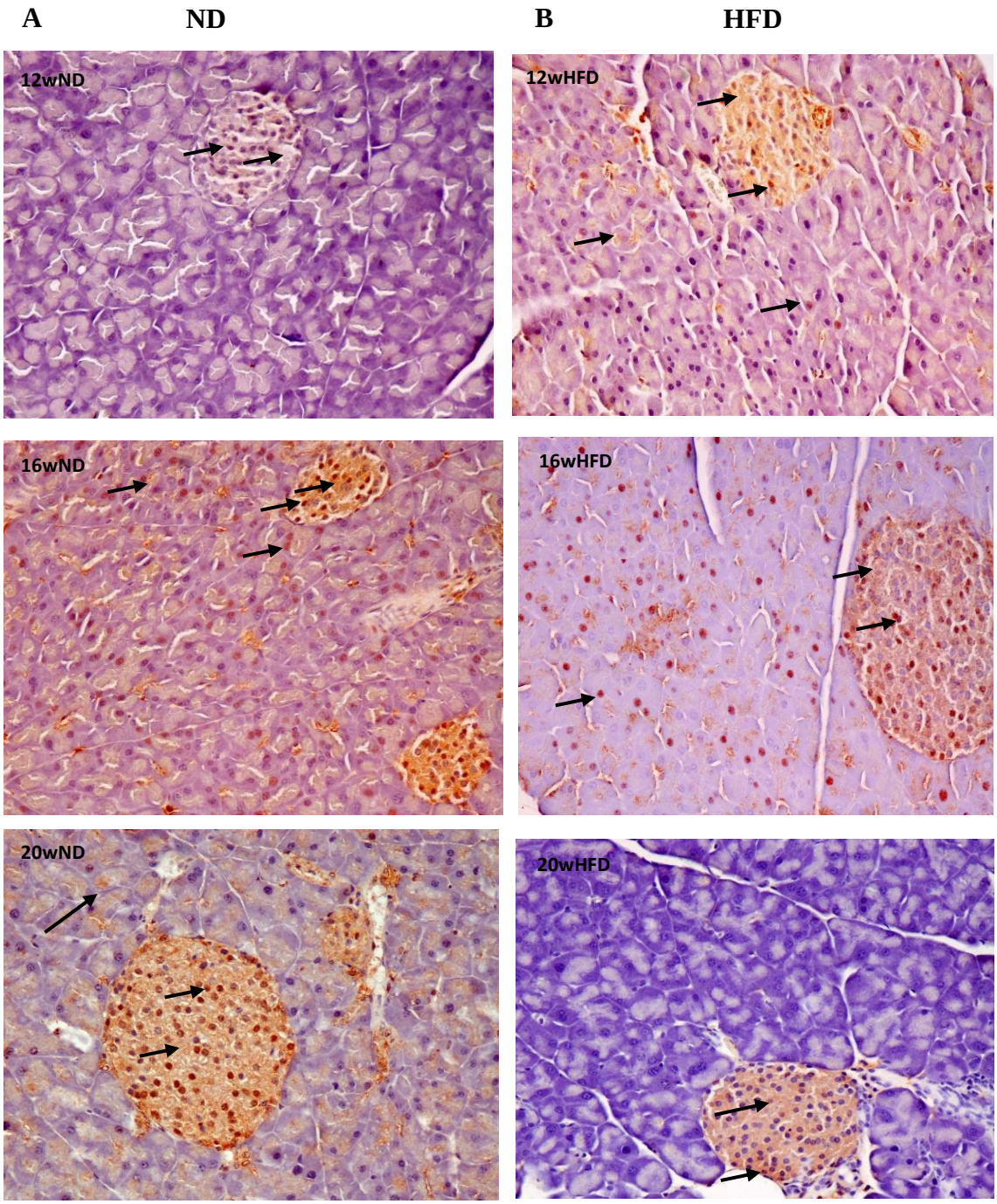

Figure 19. Representative images for the GLB1 immunohistochemistry results at weeks 12, 16, and 20 (Amplification: 100x) in mice pancreas of the (A) normal diet (ND) and the (B) high-fat diet (HFD) group (arrows: Brown in the nucleus and cytoplasm of the pancreatic islets of Langerhans and acini staining positive for GLB1). In the pancreas of the ND mice, we can see an increase in the staining of the islet's cells between weeks 12 and 20. Also, it is noticing an increase in GLB1 stained cells in the exocrine pancreas in weeks 16 and 20. In the obese pancreas, at week 12, there is already a distinguished increase in staining of pancreas cells for GLB1, comparing to the healthy mice for that age. Then, at week 20, we see a decrease in the content of GLB1 stained cells in endocrine (and also in exocrine) mice obese pancreas.

3.6.2 PCNA expression in pancreatic cells

Contrary to what it was expected, we did not observe positive islets pancreatic cells staining for this marker of proliferation, only in exocrine pancreatic cells.

To our knowledge, no studies were performed using PCNA as a proliferative pancreatic biomarker in the same experimental model used in this study. So, one of the possible explanations for our results could be a low PCNA protein expression in the islets cells of these mice. Also, PCNA is not as specific as the Ki-67 marker for cell proliferation[87]. Ki-67 monoclonal antibody to Ki-67 is reported to be extremely effective in formalin-fixed paraffin-embedded paraffin sections. KI-67 antigen expression generally correlates with cells in the mitotic state, although it is usually more sensitive to the G1, G2, and S phases in addition to the M phase of the cell cycle[88]. However, we used PCNA instead of Ki-67, due to its immediate logistical availability.

Figures 20A and *B*, shows the results for the PCNA immunohistochemistry. We do not see significant differences for the ND animals over time, however for the HFD ones it seems to be a notable decrease in proliferative exocrine pancreatic cells with age. This can be supported by the results for the quantification of PCNA stained cells (*Figure 21*) where it is showed a significant decrease for the obese subjects between week 12 and weeks 16 and 20.

Overall, these results do not inform about the proliferative state of β-cells in the two experimental diet models with age, but elucidate for a negatively influence of the ingestion of an HFD in the proliferation state of the exocrine pancreatic cells with age.

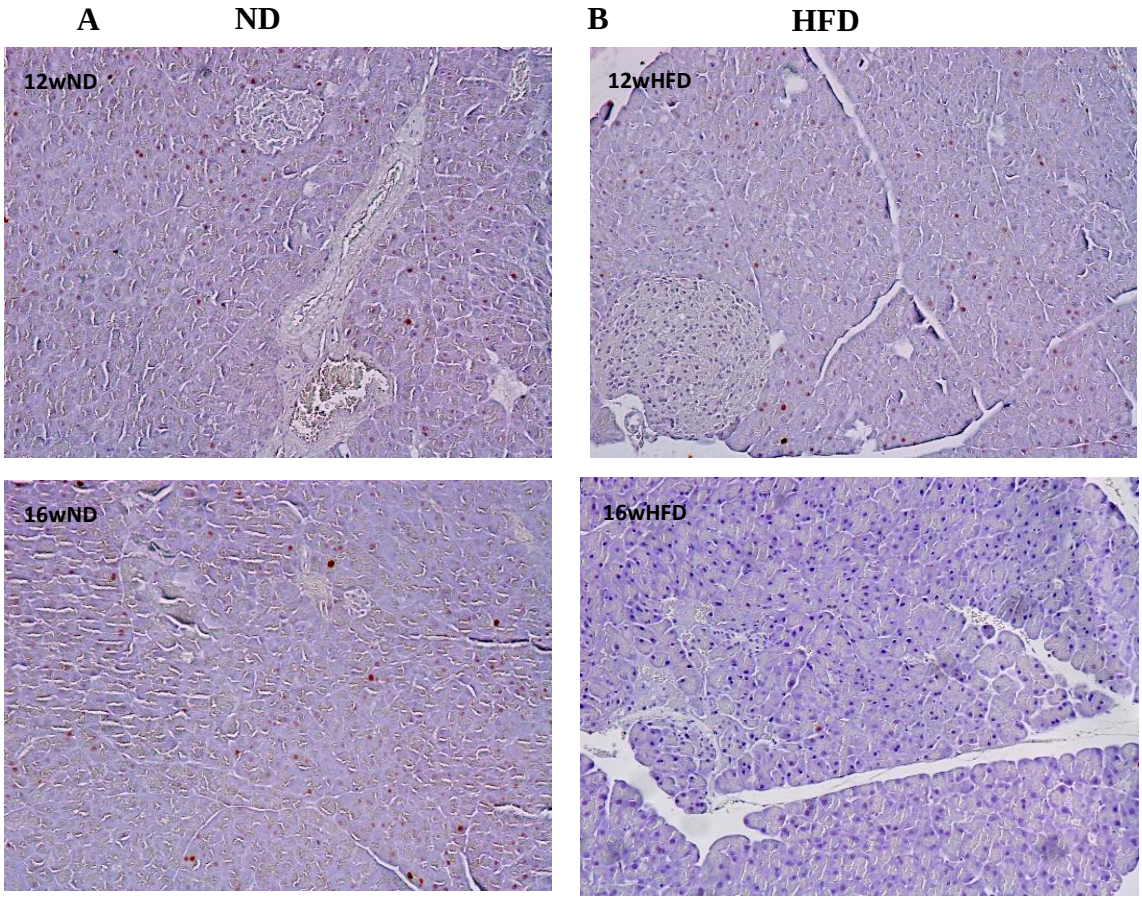

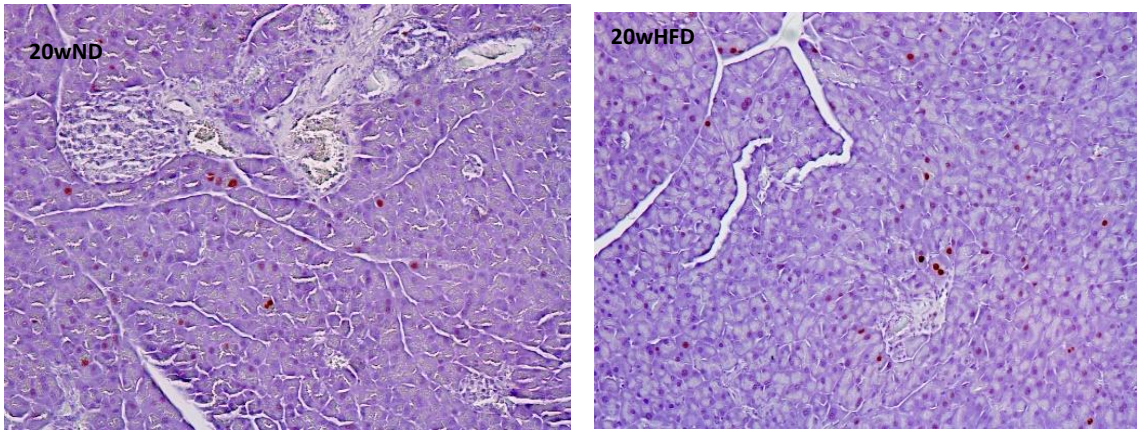

Figure 20. Representative images for the PCNA immunohistochemistry results at weeks 12, 16, and 20 (Amplification: 100x) for the (A) normal diet (ND) mice and the (B) high-fat diet (HFD) group. The red colour in the nucleus of pancreatic acini and in the nucleus of the cell of the islets of Langerhans represents the stains for PCNA positive cells. For the ND subjects, we do not see significant differences in proliferative cells on the exocrine pancreas. In the HFD group, there is a notable decreased exocrine pancreatic cells proliferation. The presented islets do not have any cell staining positive for PCNA.

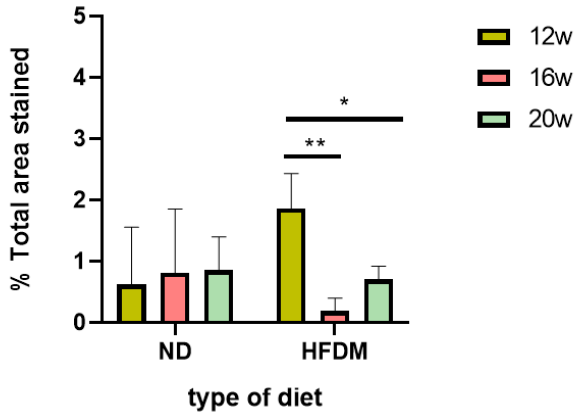

Figure 21. Proliferative pancreatic cell content in C57BL/6J mice fed with the two diets- normal diet (ND) group and high-fat diet (HFD) group- at weeks 12, 16, and 20. There is a decrease in the PCNA stained cells in the HFD group over time. At weeks 16 and 20, we see very significant decrease in proliferative acini cells, compared to the results for week 12. $P<0.05$ and $^{**}P<0.01$. P values were determined by the two-way ANOVA test, followed by the Sidak test.

3.6.3 Lipofuscin deposition in pancreatic cells

Lipofuscin accumulation in mice pancreas was assessed by the Sudan-Black-B (SBB) histochemical staining. SBB staining is widely used for the identification of lipofuscin and was recently proved to be highly specific for identification of senescent cells in paraffin-embedded tissues[48,89].

Results of SBB staining (Figure 22) reveal no pancreatic expression of LB of both studied groups. The absence of LB detection in our experimental model may be explained by the fact that lipofuscin is normally found in very old aged tissues with largely senescent content[30]. In the present study, we used adult mice.

However, these results may drive the conclusion that obesity does not influence the appearance of lipofuscin in senescent cells in the obese pancreas, at adult age.

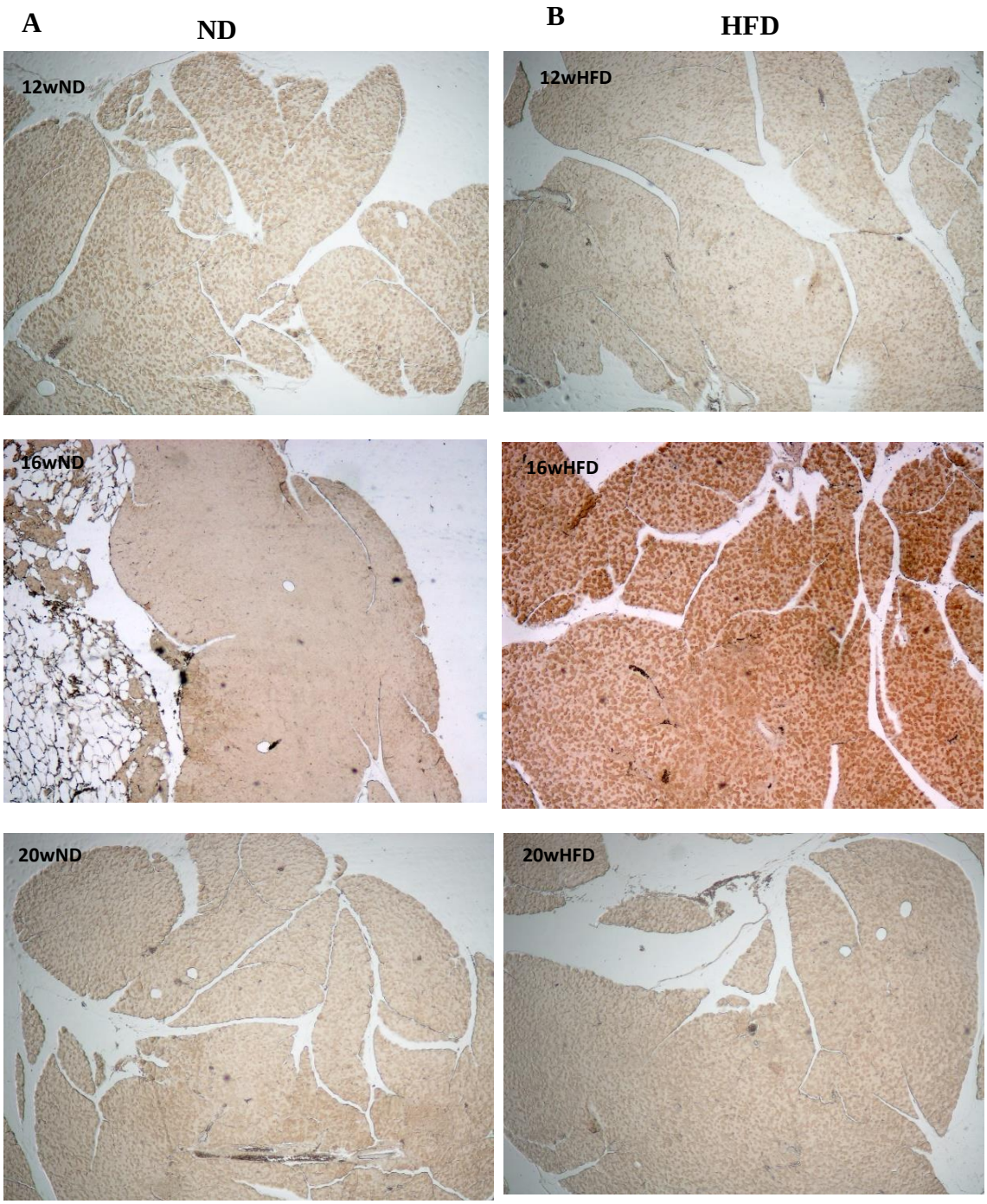

Figure 22. Representative images for the SBB staining results at weeks 12, 16, and 20 (Amplification: 40x) in mice pancreas of the (A) normal diet (ND) and the (B) high-fat diet (HFD) group. There is no LB detected.

3.7 Fibrosis

Previous studies reported that, with age, occurs an increased content in fibrosis around the acini, islets, and extracellular matrix in the healthy mice and human pancreas[45,39]. High-fat diet intake and obesity seems to anticipate the formation of fibrosis at younger ages[90].

Since we saw some differences between the groups with time in senescent content and once fibrosis is linked to the senescence, we intendent to evaluate if there is the formation of fibrosis in the adult mice at 12, 16, and 20 weeks.

To evaluate the pancreatic content of these mice in collagen fibres, Masson's Trichrome (MT) and Sirius Red (SR) stainings were performed. Evolution of collagen fibres with these two histological stainings is commonly used in paraffin-embedded tissues[91].

3.7.1 Masson Trichrome Staining

In *Figure 23*, displays the distribution of the type I collagen fibres in mice pancreas, depending on the type of diet along with the three-time points.

The ND animals showed delicate collagen fibres around the pancreatic acini, islets, and blood vessels (*Figure 23A*). We do not see notable differences in healthy mice among the 20 weeks.

For the obese animals, the TM staining results suggest an increase in the fibrosis content between weeks 12 and 16, represented by the blue stain around the acini and inside pancreatic islets (*Figure 23B)* and a decrease in the fibrotic content at week 20.

In *Figure 24*, we demonstrate the results for the fibrosis quantification in the total pancreas of ND and HFD groups. The results do not show significant differences between the ND and the HFD groups at the ages of 12, 16, and 20.

A **ND** **B** **HFD**

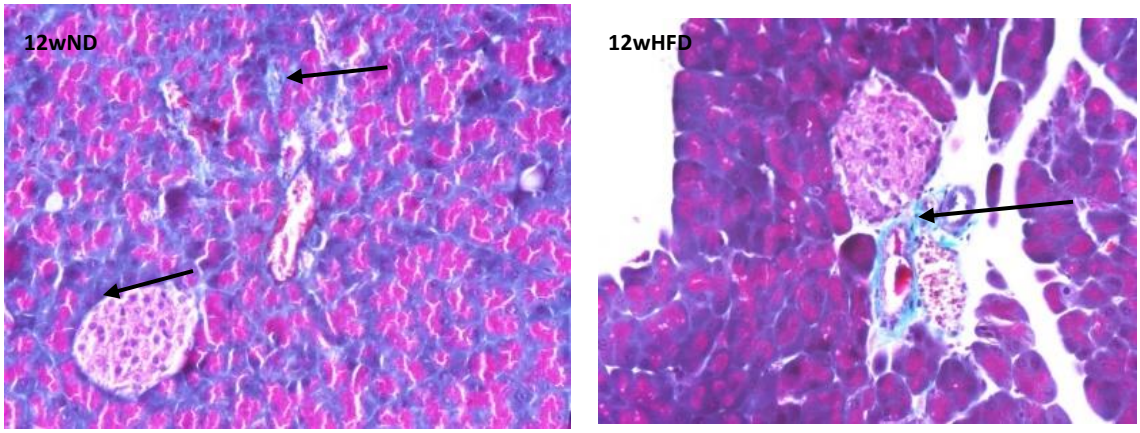

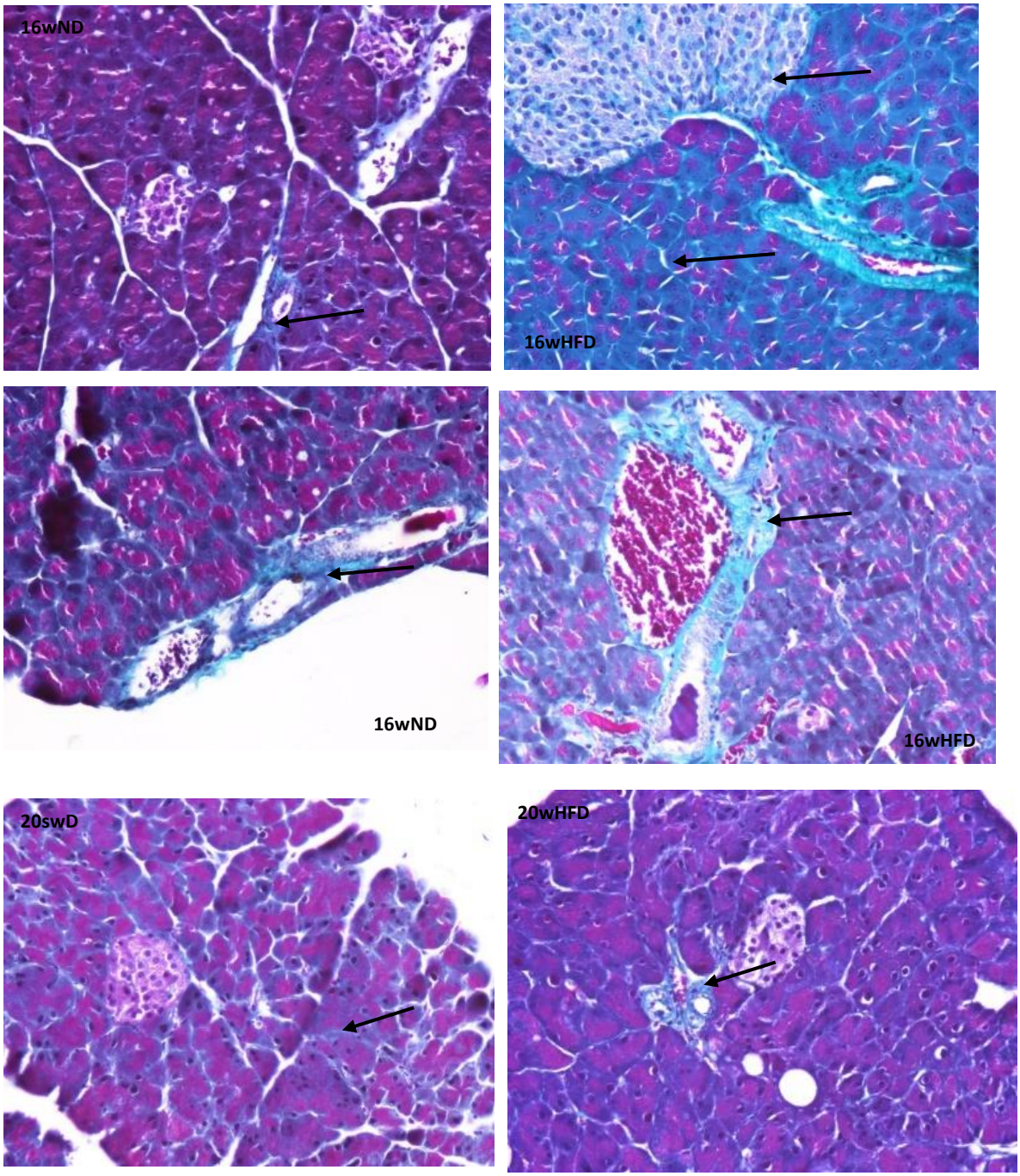

Figure 23. Representative images for the MT staining results at weeks 12, 16, and 20 (Amplification: 200x) for the pancreas of (A) the normal diet (ND) mice and (B) the high-fat diet (HFD) mice. The blue colour (arrow) around the cells of the pancreatic islets and between acini is staining for collagen fibres. For ND animals, is not observed differences in fibrosis content over time. Regarding HFD we observe an increase in fibrotic content at week 16 around the acini cells, inside the islets and around blood vessels.

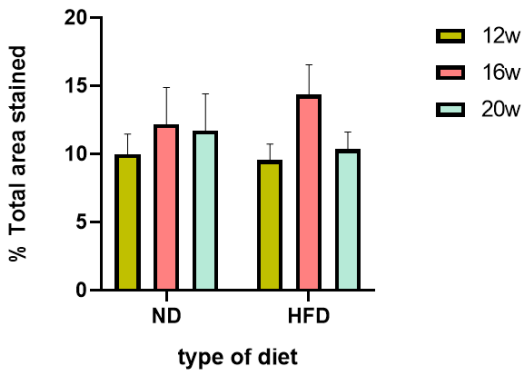

Figure 24. MT staining results for collagen deposition in C57BL/6J mice pancreas, fed with the two different diets- normal diet (ND) group and high-fat diet (HFD) group- at weeks 12, 16, and 20. There are no significant results.

3.7.2 Sirius Red Staining

Once the results from the MT staining were not significant but suggested a variation in the fibrotic content in obese mice, we decided to perform the Sirius red staining, which is commonly used as a measure of collagen deposition in the pancreas[92]. The results are presented below in *Figures 25* and *26*.

Regarding the pancreas from normoponderal mice, no significant differences were found along 3 weeks (*Figure 26*). But a slight increase in fibrotic content around the pancreatic islets and acini is suggested by *Figure 25A*.

In HFD mice, we see a significant increase in collagen deposition at week 16, compared to the results of week 12, and then at week 20, it seems to occur a decrease in collagen fibres content, a result supported by *Figure 25B*

The SR staining results were coherent with the ones obtained in the MT staining.

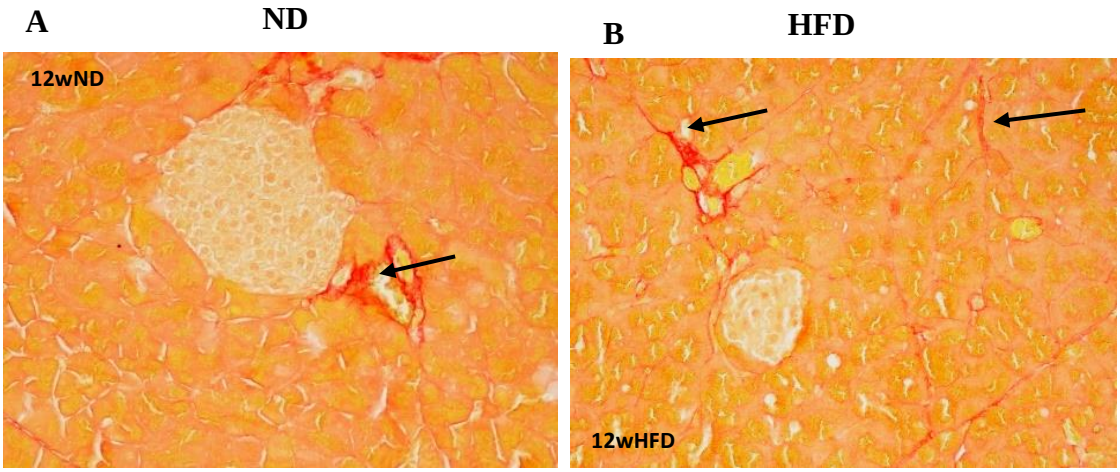

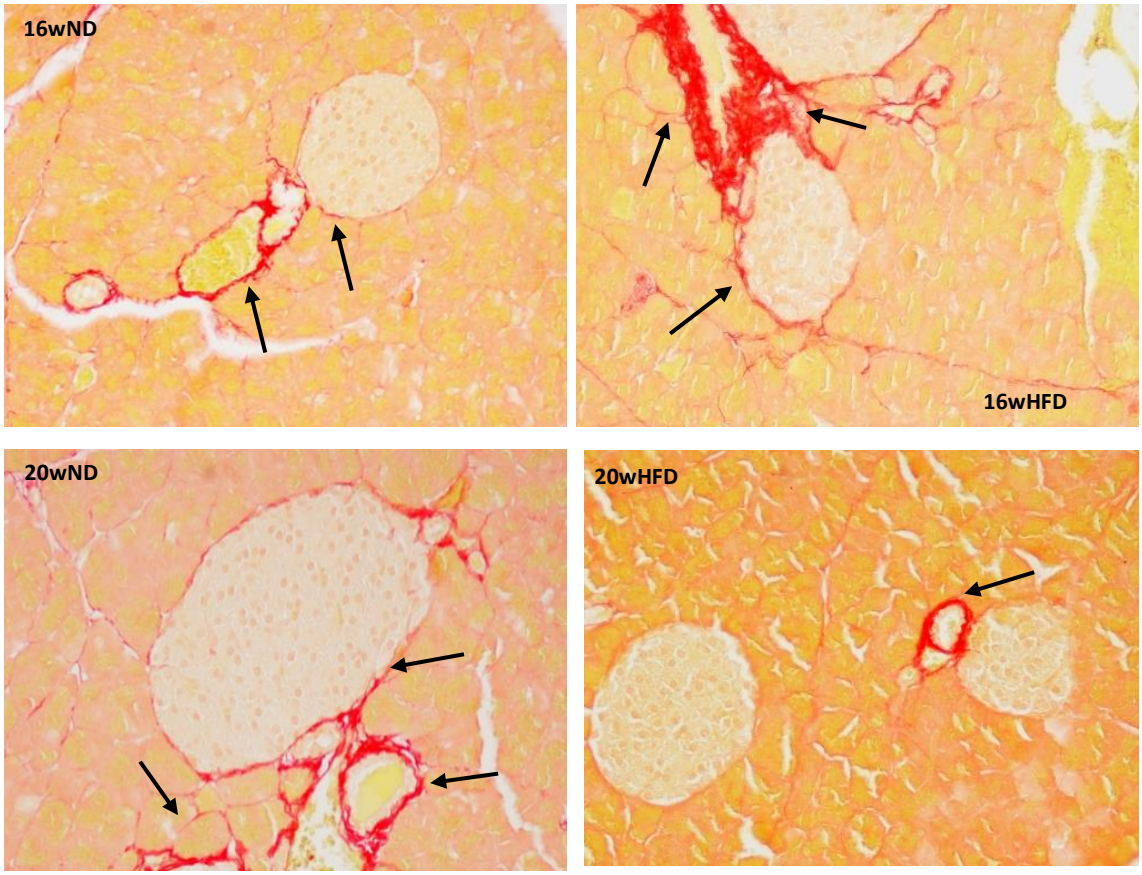

Figure 25. Representative images for the SR staining results at weeks 12, 16, and 20 (Amplification: 200x) for the (A) normal diet (ND) mice and the (B) high-fat diet (HFD) group (arrow: collagen fibres in red around the pancreatic acini, islands, β-cells, and blood vessels). In the ND animals, it seems to exist an increase in fibrosis at week 20, with larger collagen fibres around the acini and islets. In the obese pancreas, at week 16, is observed an increase in the fibrotic content.

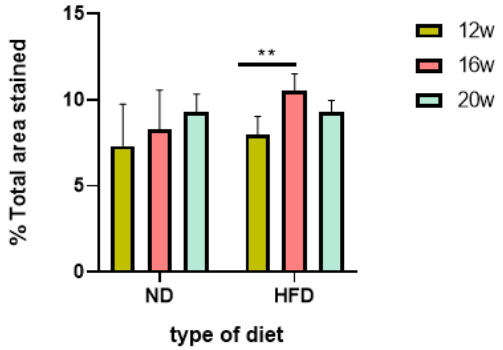

Figure 26. SR staining results for collagen deposition in C57BL/6J mice pancreas, fed with the two different diets- normal diet (ND) group and high-fat diet (HFD) group- at weeks 12, 16, and 20. In the HFD group, there is a significant increase in collagen deposition between weeks 12 and 16. -***P*<0.01. P values were determined by the two-way ANOVA test, followed by the Sidak test.

The assays performed for evaluation of the fibrosis formation in both ND and HFD groups along time suggest an increase in the fibrotic content in the HFD group at week 16, where are reported the clearest negative effects of obesity. However, following the results for HFD mice at week 20, we expected to observe a significant decrease in the collagen fibres deposition at that time. Yet, these results only regard the fibrotic content in the total pancreas i.e., we did not observe the fibrotic content particularly in islets cells, so we cannot draw conclusions about the fibrosis relationship with the cellular senescent process and its influence on β-cells function. Thus, more experiments are required to better understand the impact of the diet in collagen deposition with age and its influence on β-cells function.

3.8 Amyloid deposits in β-cells

Amyloid deposits formed in pancreatic islets of T2D patients and have been associated with loss of β-cell mass and function with the progression of this disease[93].

Congo red histological staining was used to identify the amyloid deposits in pancreatic β-cells of the ND and HFD mice at weeks 12, 16, and 20. The results are present in *Figure 27* and no amyloid deposits were detected in both groups with time.

These results can be supported by fact that the mouse and rat islet amyloid polypeptide (IAPP) differ structurally from the human protein, maintaining the protein soluble form, preventing aggregation. So, mouse and rat models currently used for obese and T2D studies cannot form amyloid deposits in islets cells.

A **ND** **B** **HFD**

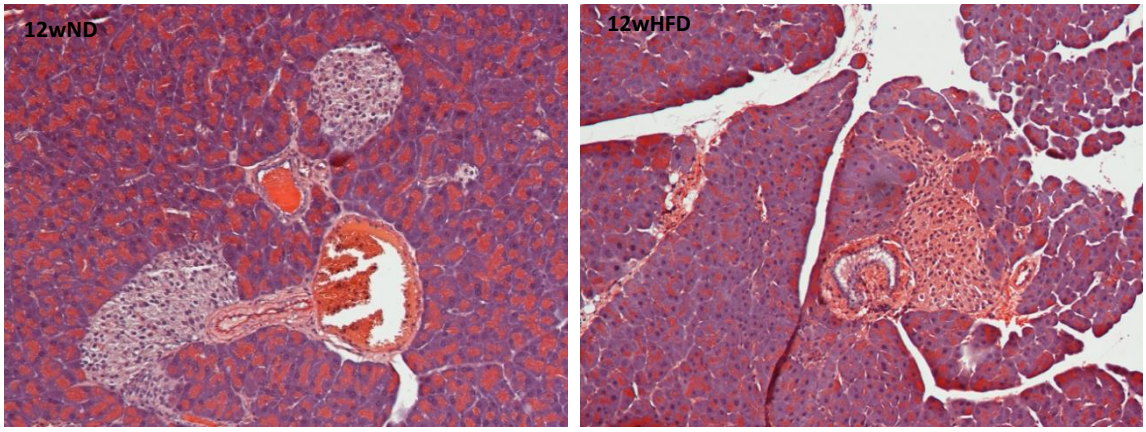

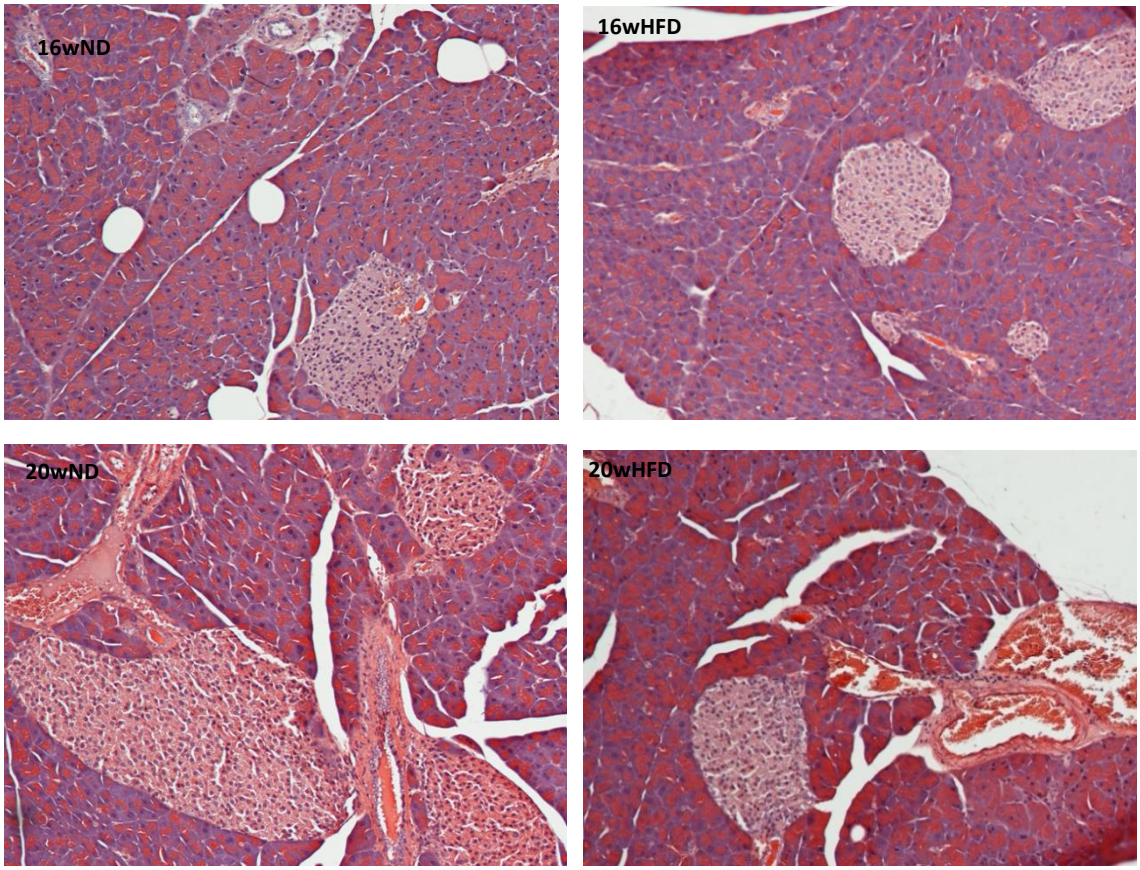

Figure 27. Representative images for the Congo red staining results at weeks 12, 16, and 20 (Amplification: 40x) in mice pancreas of the (A) normal diet (ND) and the (B) high-fat diet (HFD) group. There are no amyloid deposits detected in β-cells.

4. Conclusion and Future Perspectives

Ageing is a multi-factorial and inevitable biological process that promotes progressive deterioration across multiple organs, resulting in tissue dysfunction[1]. Nowadays, there is an increased interest in the study of the ageing process and its metabolic features, however, little is known about the ageing process of the pancreas. Obesity is a metabolic disease, that affects the well-function of the pancreatic β-cells, contributing to insulin resistance. Data considering the age-related changes in obesity disease has elucidated for the fact that obesity could be considered a condition of premature metabolic dysfunction resembling ageing and induce premature cell senescence[94,95,96].

In this research project, we aimed to evaluate the effects of diet-induced obesity in some of the age-related pancreatic alterations in adult mice, with time.

Here, two main conclusions may be achieved.

Firstly, it is suggested an alteration of the total pancreatic function and, in specific, for the β-cells function, in ND animals, with age. Even at an adult phase, we observed an increase in β-cells senescence followed by decreased insulin production and increase fibrogenesis, which may reinforce the idea that cellular senescence is the mechanism behind age-related β-cell dysfunction[51].

Second, we notice a pancreatic metabolic protection against obesity and age-related consequences in obese mice at the age of 7 months (middle-age mice). At week 16, there is an alteration in the pancreatic cells, typically from obese pancreatic metabolic changes, i.e., increased islets size, increased insulin production, increased β-cell senescence, and increased collagen fibres deposition. Then at week 20, the exocrine and endocrine pancreatic architecture is restored, followed by a decrease in pancreatic cell senescence. These results follow the ones obtained in recent studies where a reverse of the obese effects in adipose and liver tissues in middle-aged and advanced-aged animals was observed[97,98].

Herein, we suggest that the reverse of the pancreatic obese effects may be achieved in an adult phase. However, the mechanisms involved in this metabolic twist are not fully understood. At the age of 1-year obese mice have the capacity to respond with β-cell proliferation to pancreatic damage, with no regenerative response after 1-year. Probably the mechanisms involved in β-cell turnover are the key to reversing the age-related consequences in obese mice, at an adult and middle-aged, with an increase in β-cell proliferation faced to the formation of senescent β-cells.

Some limitations can be pointed in this research project. Starting with the experimental model, it was predetermined and used for previous studies, which explains the fact of the animals used in this experimental project are not considered as old. Additionally, animal monitoring was accessed by researchers that were not involved in the current project. Thus, for this experimental project, we just had access to the paraffin-embedded blocks and not the blood samples or tissue lysate, which prevents us to perform other analysis to the blood, as the evaluation of proinflammatory markers.

Thereby, despite these promising results, further research is needed. First, the study should be extended to older ages, to evaluate the age effects in the obese pancreas of middle and advanced-aged mice. Also, it would be helpful to obtain results for the proliferative status of the β-cells with time. For that, Ki-67 proliferative marker should be used and the results must be compared to the number of SA- β-gal positive β-cells. Then, the evaluation of the expression of other senescent markers could be helpful to elucidate the senescent cellular mechanisms activated by the two distinct diets. Senescent markers such as p16 and p21 cell-cycle inhibitors should be accessed; lipofuscin detection should be achieved in older mice, and SA- β-gal activity assay should be performed in the tissue, to confirm the results obtained for the GLB1-positive cells in the paraffine-embedded sections[99,25]; also, in order to understand how obesity can protect the HFD mice with age, assays focusing the type of metabolism undergoing β-pancreatic cells in obese subjects and the changes suffered from age should be performed and achieved by metabolomics analysis.

5. References

1. Kirkwood, T. B. L. Understanding the odd science of aging. *Cell* vol. 120 437–447 (2005).
2. Klass, M. R. A method for the isolation of longevity mutants in the nematode Caenorhabditis elegans and initial results. *Mech. Ageing Dev.* **22**, 279–286 (1983).
3. López-Otín, C., Blasco, M. A., Partridge, L., Serrano, M. & Kroemer, G. The hallmarks of aging. *Cell* vol. 153 1194 (2013).
4. Mchugh, D. & Gil, J. Senescence and aging : Causes , consequences , and therapeutic avenues. *J. Cell Biol.* **217**, 65–77 (2018).
5. Coppé, J. P. *et al.* A human-like senescence-associated secretory phenotype is conserved in mouse cells dependent on physiological oxygen. *PLoS One* **5**, e9188 (2010).
6. Storer, M. *et al.* XSenescence is a developmental mechanism that contributes to embryonic growth and patterning. *Cell* **155**, 1119 (2013).
7. Demaria, M. *et al.* An essential role for senescent cells in optimal wound healing through secretion of PDGF-AA. *Dev. Cell* **31**, 722–733 (2014).
8. Collado, M. & Serrano, M. Senescence in tumours: Evidence from mice and humans. *Nature Reviews Cancer* vol. 10 51–57 (2010).
9. Kuilman, T., Michaloglou, C., Mooi, W. J. & Peeper, D. S. The essence of senescence. *Genes Dev.* **24**, 2463–2479 (2010).
10. Salama, R., Sadaie, M., Hoare, M. & Narita, M. Cellular senescence and its effector programs. *Genes and Development* vol. 28 99–114 (2014).
11. Davalli, P. *et al.* ROS , Cell Senescence , and Novel Molecular Mechanisms in Aging and Age-Related Diseases. *Oxid. Med. Cell. Longev.* **2016**, 1–18 (2016).
12. Maduro, A. T., Luís, C. & Soares, R. Ageing, cellular senescence and the impact of diet: an overview. *Porto Biomed. J.* **6**, e120 (2021).
13. Bennett G Childs1, Matej Durik2, Darren J Baker1, 2, and Jan M van Deursen1, 2. Cellular senescence in aging and age-related disease: from mechanisms to therapy Bennett. *Nat. Med.* **21**, 1424–1435 (2015).
14. Dimri, G. P. *et al.* A biomarker that identifies senescent human cells in culture and in aging skin in vivo. *Natl. Acad. Sci. United States Am.* **92**, 9363–9367 (1995).
15. Mann, D. M. A., Yates, P. O. & Stamp, J. E. The relationship between lipofuscin pigment and ageing in the human nervous system. *J. Neurol. Sci.* **37**, 83–93 (1978).
16. Childs, B. G., Baker, D. J., Kirkland, J. L., Campisi, J. & Deursen, J. M. Van. Senescence and apoptosis : dueling or complementary cell fates ? *EMBO Rep.* **15**, 1139–1153 (2014).
17. Pole, A. Oxidative stress , cellular senescence and ageing. *AIMS Mol. Sci.* **3**, 300–324 (2016).
18. Ziegler, D. V., Wiley, C. D. & Velarde, M. C. Mitochondrial effectors of cellular senescence: Beyond the free radical theory of aging. *Aging Cell* **14**, 1–7 (2015).
19. Liguori, I. *et al.* Oxidative stress, aging, and diseases. *Clinical Interventions in Aging* vol. 13 757–772 (2018).
20. Siderakis, M. & Tarsounas, M. Telomere regulation and function during meiosis. *Chromosom. Res.* **15**, 667–679 (2007).
21. Sanders, J. L. & Newman, A. B. Telomere length in epidemiology: A biomarker of aging, age-related disease, both, or neither? *Epidemiol. Rev.* **35**, 112–131 (2013).
22. Chandrasekaran, A., Sosa, P. & Melendez, J. A. Redox Biology Redox control of senescence and age-related disease. *Redox Biol.* **11**, 91–102 (2017).
23. Shay, J. Hallmarks of telomers in ageing research. *J. Pathol.* **211**, 114–123 (2007).
24. Cristofalo, V. J., Lorenzini, A., Allen, R. G., Torres, C. & Tresini, M. Replicative senescence: A critical review. *Mech. Ageing Dev.* **125**, 827–848 (2004).
25. Lee, B. Y. *et al.* Senescence-associated β-galactosidase is lysosomal β-galactosidase. *Aging Cell* **5**, 187–195 (2006).
26. Paradis, V. *et al.* Replicative senescence in normal liver, chronic hepatitis C, and hepatocellular carcinomas. *Hum. Pathol.* **32**, 327–332 (2001).
27. Price, J. S. *et al.* The role of chondrocyte senescence in osteoarthritis. *Aging Cell* **1**, 57–65 (2002).
28. Moreno-García, A., Kun, A., Calero, O., Medina, M. & Calero, M. An overview of the

role of lipofuscin in age-related neurodegeneration. *Front. Neurosci.* **12**, 1–13 (2018).
29. Brunk, U. T. & Terman, A. Lipofuscin: Mechanisms of age-related accumulation and influence on cell function. *Free Radic. Biol. Med.* **33**, 611–619 (2002).
30. Jung, T., Bader, N. & Grune, T. Lipofuscin: Formation, distribution, and metabolic consequences. *Ann. N. Y. Acad. Sci.* **1119**, 97–111 (2007).
31. Mondal, S. Pigments and Minerals. *Man. Histol. Tech.* 63–63 (2017) doi:10.5005/jp/books/13001_11.
32. Matsuda, Y. Age-related pathological changes in the pancreas. *Front. Biosci. - Elit.* **10**, 137–142 (2018).
33. Merino, P. L. H. Developmental biology of the pancreas. *Cell Biochem. Biophys.* **40**, 127–142 (2004).
34. Stamm, B. H. Incidence and diagnostic significance of minor pathologic changes in the adult pancreas at autopsy:. A systematic study of 112 autopsies in patients without known pancreatic disease. *Hum. Pathol.* **15**, 677–683 (1984).
35. Caglar, V. *et al.* Age-related volumetric changes in pancreas: A stereological study on computed tomography. *Surg. Radiol. Anat.* **34**, 935–941 (2012).
36. Sato, T. *et al.* Age-related changes in normal adult pancreas: MR imaging evaluation. *Eur. J. Radiol.* **81**, 2093–2098 (2012).
37. Makay, O. *et al.* Fat replacement of the malignant pancreatic tissue after neoadjuvant therapy. *Int. J. Clin. Oncol.* **15**, 88–92 (2010).
38. Matsuda, Y. *et al.* The prevalence and clinicopathological characteristics of high-grade pancreatic intraepithelial neoplasia autopsy study evaluating the entire pancreatic parenchyma. *Pancreas* **46**, 658–664 (2017).
39. Detlefsen, S., Sipos, B., Feyerabend, B. & Klöppel, G. Pancreatic fibrosis associated with age and ductal papillary hyperplasia. *Virchows Arch.* **447**, 800–805 (2005).
40. Riccillo, F. L., Bracamonte, M. I., Cónsole, G. M. & Gómez Dumm, C. L. A. Histomorphological and quantitative immunohistochemical changes in the rat pancreas during aging. *Biocell* **28**, 127–134 (2004).
41. Kehm, R. *et al.* Age-related oxidative changes in pancreatic islets are predominantly located in the vascular system. *Redox Biol.* **15**, 387–393 (2018).
42. Tokuyama, T. *et al.* Expression of human islet amyloid polypeptide/amylin impairs insulin secretion in mouse pancreatic β cells. *Metabolism.* **46**, 1044–1051 (1997).
43. Swenne, I. Effects of aging on the regenerative capacity of the pancreatic B-cell of the rat. *Diabetes* **32**, 14–19 (1983).
44. Maedler, K. *et al.* Aging correlates with decreased β-cell proliferative capacity and enhanced sensitivity to apoptosis: A potential role for fas and pancreatic duodenal homeobox-1. *Diabetes* **55**, 2455–2462 (2006).
45. Wang, L. Z. S. Pancreatic senescence and its clinical manifestations. *Aging Med.* **3**, 48–52 (2020).
46. Cerf, M. E. Beta cell dysfunction and insulin resistance. *Front. Endocrinol. (Lausanne).* **4**, 1–12 (2013).
47. Reers, C. *et al.* Impaired islet turnover in human donor pancreata with aging. *Eur. J. Endocrinol.* **160**, 185–191 (2009).
48. Cnop, M. *et al.* The long lifespan and low turnover of human islet beta cells estimated by mathematical modeling of lipofuscin accumulation. *Diabetologia* **53**, 321–330 (2010).
49. Cnop, M. *et al.* Endocytosis of low-density lipoprotein by human pancreatic β cells and uptake in lipid-storing vesicles, which increase with age. *Am. J. Pathol.* **156**, 237–244 (2000).
50. Krishnamurthy, J. *et al.* p16INK4a induces an age-dependent decline in islet regenerative potential. *Nature* **443**, 453–457 (2006).
51. Burton, D. G. A. & Faragher, R. G. A. Cellular senescence: from growth arrest to immunogenic conversion. *Age (Omaha).* **37**, 1–19 (2015).
52. Matsuda, Y. Age-related morphological changes in the pancreas and their association with pancreatic carcinogenesis. *Pathol. Int.* **69**, 450–462 (2019).
53. Choi, J. W., Pai, S. H. & Kim, S. K. Associations between total body fat and serum lipid

concentrations in obese human adolescents. *Ann. Clin. Lab. Sci.* **32**, 271–278 (2002).
54. SIMOPOULOS, A. P. Characteristics of Obesity: An Overview. *Ann. N. Y. Acad. Sci.* **499**, 4–13 (1987).
55. Must, A. *et al.* The Disease Burden Associated With Overweight and Obesity. *J. Am. Med. Assoc.* **282**, 1523–1529 (1999).
56. Ahima, R. S. Connecting obesity, aging and diabetes. *Nature Medicine* vol. 15 996–997 (2009).
57. Ritov, V. B. *et al.* Mitochondrial deficiency in Obesity and Type 2 Diabetes. *Diabetes* **54**, 8–14 (2004).
58. Schafer, M. J. *et al.* Cellular senescence: Implications for metabolic disease. *Mol. Cell. Endocrinol.* **455**, 93–102 (2018).
59. Schafer, M. J., Miller, J. D. & LeBrasseur, N. K. Cellular senescence: Implications for metabolic disease. *Mol. Cell. Endocrinol.* **455**, 93–102 (2017).
60. Sone, H. & Kagawa, Y. Pancreatic beta cell senescence contributes to the pathogenesis of type 2 diabetes in high-fat diet-induced diabetic mice. *Diabetologia* **48**, 58–67 (2005).
61. Rebours, V. *et al.* Obesity-induced pancreatopathy in rats is reversible after bariatric surgery. *Sci. Rep.* **8**, 1–11 (2018).
62. Helman, A. *et al.* p16 Ink4a-induced senescence of pancreatic beta cells enhances insulin secretion. *Nat. Med.* **22**, 412–420 (2016).
63. Schneider, C. A., Rasband, W. S. & Eliceiri, K. W. NIH Image to ImageJ: 25 years of image analysis. *Nature Methods* vol. 9 671–675 (2012).
64. Lamprecht, M. R., Sabatini, D. M. & Carpenter, A. E. CellProfiler™: Free, versatile software for automated biological image analysis. *Biotechniques* **42**, 71–75 (2007).
65. Tollemar, V. *et al.* Quantitative chromogenic immunohistochemical image analysis in cellprofiler software. *Cytom. Part A* **93**, 1051–1059 (2018).
66. Ewald, J. A. *et al.* Androgen deprivation induces senescence characteristics in prostate cancer cells in vitro and in vivo. *Prostate* **73**, 337–345 (2013).
67. Aguayo-Mazzucato, C. *et al.* β Cell Aging Markers Have Heterogeneous Distribution and Are Induced by Insulin Resistance. *Cell Metab.* **25**, 898-910.e5 (2017).
68. Mauvais-Jarvis, F. Sex differences in metabolic homeostasis, diabetes, and obesity. *Biol. Sex Differ.* **6**, 1–9 (2015).
69. Rossmeisl, M., Rim, J. S., Koza, R. A. & Kozak, L. P. Variation in type 2 diabetes - Related traits in mouse strains susceptible to diet-induced obesity. *Diabetes* **52**, 1958–1966 (2003).
70. Zhou, X. & Hansson, G. K. Effect of Sex and Age on Serum Biochemical Reference Ranges in C57BL/6J Mice. *Comp. Med.* **54**, 176–178 (2004).
71. Wei P., Lane P.H., Lane B.J., Padanilam B.J., S. S. C. Glomerular structural and functional changes in a high-fat diet mouse model of early-stage Type 2 diabetes. *Diabetologia* **47**, 1541–1549 (2004).
72. Ahre, B. W. M. S. The High-Fat Diet–Fed Mouse. *Diabetes* **53**, 215–219 (2004).
73. Burcelin, M. Y. *et al.* Heterogeneous metabolic adaptation of C57BL / 6J mice to high-fat diet. *Am. J. Physiol. - Endocrinol. Metab.* **282**, 834–842 (2001).
74. Eisinger, K. *et al.* Lipidomic analysis of serum from high fat diet induced obese mice. *Int. J. Mol. Sci.* **15**, 2991–3002 (2014).
75. Slavin, B. G., Zarow, C. & Warden, C. H. Morphometrical Analyses of Pancreatic Islets in the BSB Mouse Model of Obesity. *Anat. Rec.* **293**, 108–116 (2010).
76. Fischer, G. *et al.* A morphological and immunohistochemical investigation of endocrine pancreata from obese ob + / ob + mice. *Acta Histochem.* **90**, 93–101 (1991).
77. Warden, C. H. An Overview of Etiology and Treatment. *Pediatr. Clin. North Am.* **44**, 339–359 (1997).
78. Dor, Y., Brown, J., Martinez, O. I. & Melton, D. A. Adult pancreatic β-cells are formed by self-duplication rather than stem-cell differentiation. *Nature* **429**, 41–46 (2004).
79. Dor, Y. & Melton, D. A. Pancreatic Stem Cells. *Handb. Stem Cells* **2**, 513–520 (2004).
80. Bonner-Weir, S. *et al.* The pancreatic ductal epithelium serves as a potential pool of progenitor cells. *Pediatr. Diabetes, Suppl.* **5**, 16–22 (2004).

81. Brereton, M. F. *et al.* Hyperglycaemia induces metabolic dysfunction and glycogen accumulation in pancreatic β-cells. *Nat. Commun.* **7**, 1–15 (2016).
82. Navina, S. *et al.* Lipotoxicity causes multisystem organ failure and exacerbates acute pancreatitis in obesity. *Sci. Transl. Med.* **3**, (2011).
83. Afghani, E. Introduction to Pancreatic Disease: Chronic Pancreatitis. *Am. Pancreat. Assoc.* 1–9 (2015).
84. Surwit, R. S., Kuhn, C. M., Cochrane, C., McCubbin, J. A. & Feinglos, M. N. Diet-Induced Type II Diabetes in C57BL/6J Mice. *Diabetes* **37**, 1163–1167 (1988).
85. Surwit, R. S. *et al.* Differential effects of fat and sucrose on the development of obesity and diabetes in C57BL/6J and A J mice. *Metabolism* **44**, 645–651 (1995).
86. Faragher, Richard G A, Dominick G, B. A. Obesity and type-2 diabetes as inducers of premature cellular senescence and ageing. *Biogerontology* **19**, 447–459 (2018).
87. Bologna-Molina, R., Mosqueda-Taylor, A., Molina-Frechero, N., Mori-Estevez, A. D. & Sánchez-Acuña, G. Comparison of the value of PCNA and Ki-67 as markers of cell proliferation in ameloblastic tumors. *Med. Oral Patol. Oral Cir. Bucal* **18**, (2013).
88. Lloyd, R. V. Utility of Ki-67 as a prognostic marker in pancreatic endocrine neoplasms. *Am. J. Clin. Pathol.* **109**, 245–247 (1998).
89. Evangelou, K. & Gorgoulis, V. G. Sudan black B, the specific histochemical stain for lipofuscin: A novel method to detect senescent cells. *Methods Mol. Biol.* **1534**, 111–119 (2017).
90. Lostutter T.W., Lewis M.A.,Concronce JM., Neighbors C., L. M. . High Fat, High Calorie Diet Promotes Early Pancreatic Neoplasia in the Conditional KrasG12D Mouse Model. *Bone* **23**, 1–7 (2014).
91. Matsuda, A. *et al.* Pancreatic fat accumulation, fibrosis, and acinar cell injury in the zucker diabetic fatty rat fed a chronic high-fat diet. *Pancreas* **43**, 735–743 (2014).
92. Lópex-De León, A., Rojkind, M. Micromethod for Collagen and Total Protein Determination in Formalin-fixed. *J. Histochem. Cytochem.* **33**, 737–743 (1985).
93. Höppener, J. W. M. *et al.* Extensive islet amyloid formation is induced by development of Type II diabetes mellitus and contributes to its progression: Pathogenesis of diabetes in a mouse model. *Diabetologia* **42**, 427–434 (1999).
94. Tchkonia, T. *et al.* Fat tissue, aging, and cellular senescence. *Aging Cell* **9**, 667–684 (2010).
95. Burt Solorzano, C. M. & McCartney, C. R. Obesity and the pubertal transition in girls and boys. *Reproduction* **140**, 399–410 (2010).
96. Niemann, B. *et al.* Obesity induces signs of premature cardiac aging in younger patients: The role of mitochondria. *J. Am. Coll. Cardiol.* **57**, 577–585 (2011).
97. Moreno-Fernandez, M. E. *et al.* Aging mitigates the severity of obesity-associated metabolic sequelae in a gender independent manner. *Nutr. Diabetes* **11**, (2021).
98. Vercalsteren, E. *et al.* Advanced-age C57BL/6JRj mice do not develop obesity upon western-type diet exposure. *Adipocyte* **8**, 105–113 (2019).
99. Sara M. Ahmed, Shimaa E. Elshenawy, Sara Sedky, Ahmed O. Elmehrath & Nagwa El-Badri1. Pancreatic β-Cell Senescence: Mechanisms and Association with Diabetes. *Eur. Med. J.* 59–72 (2020).

6. Supporting Information

S1- CellProfiler pipeline model for histochemical and immunohistochemical quantification

1. Insert images

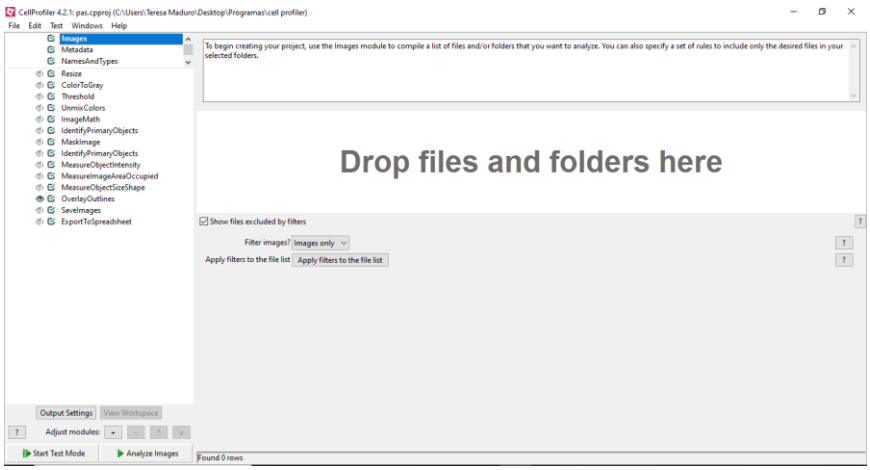

2. Decrease image size

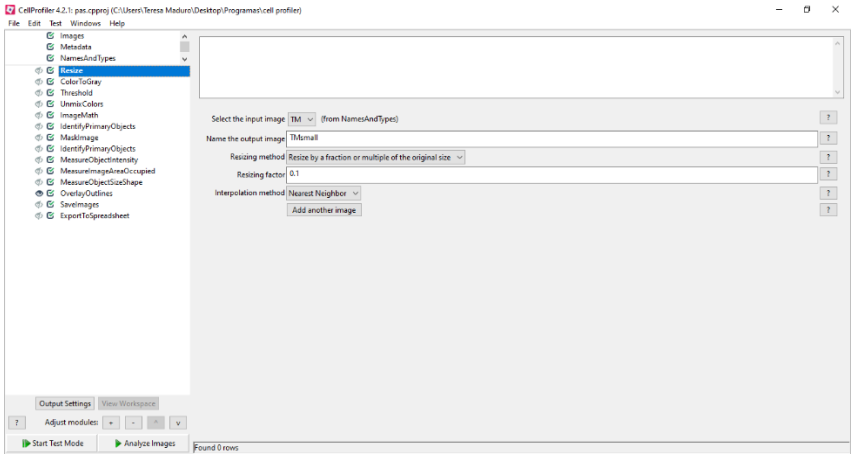

3. Insert the stains that are visible in the images

a) To PAS staining: PAS and hematoxilyn;
b) To MT staining: Light-green, hematoxylin, Celestin blue;
c) To SR staining: Fast red and orange;
d) To immunohistochemistry assays: DAB and hematoxilyn.

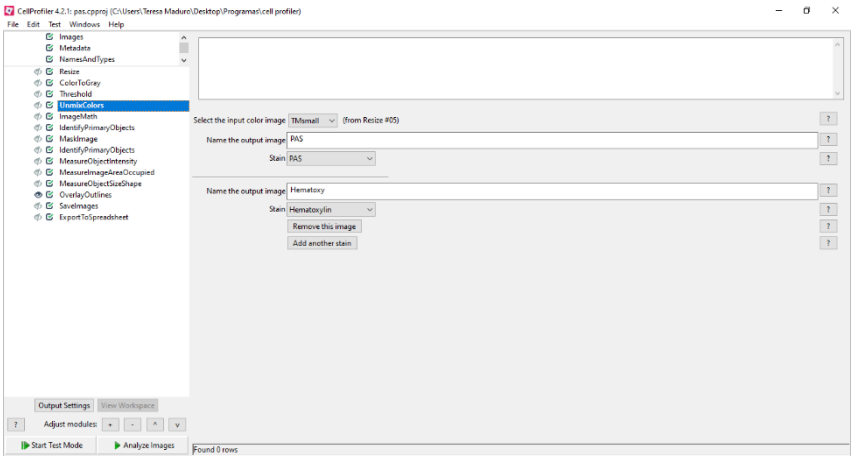

4. Remove the background colour to the stain that we want to quantify

    a) PAS staining: remove hematoxilyn to PAS
    b) MTT staining: remove hematoxylin and Celestin blue to light green
    c) SR staining: remove orange to fast red
    d) Immunohistochemistry assays: remove hematoxylin to DAB

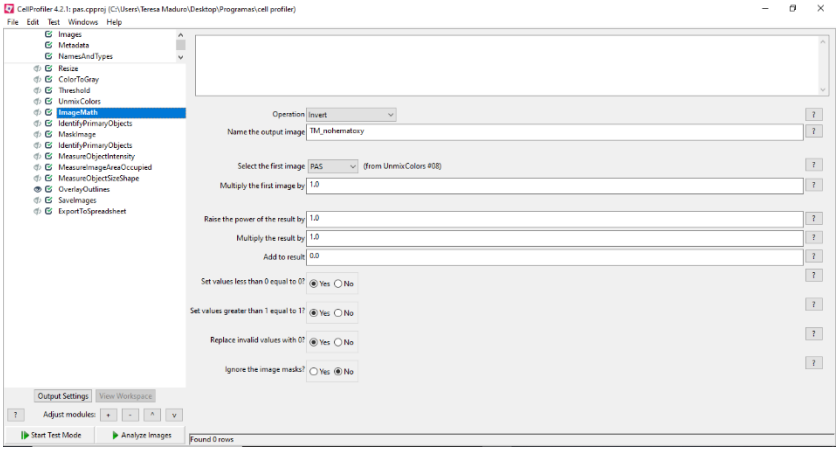

5. Identify the stain to be quantified

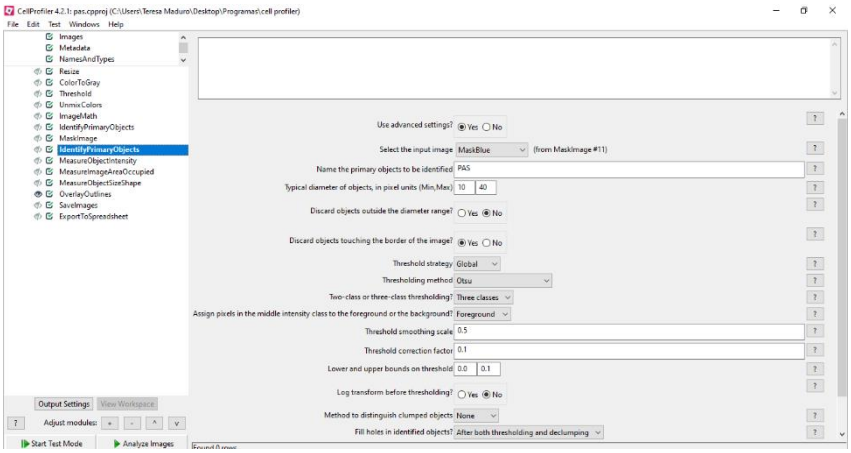

6. Stain intensity measurement

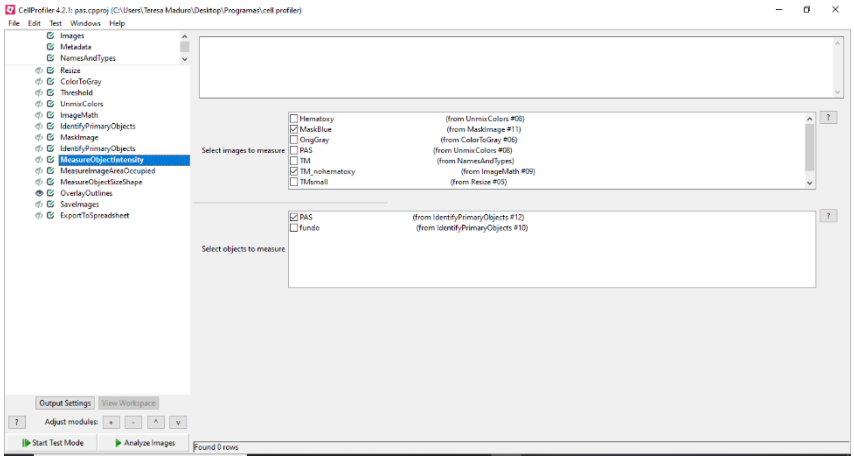

7. Measurement of area occupied for the stain

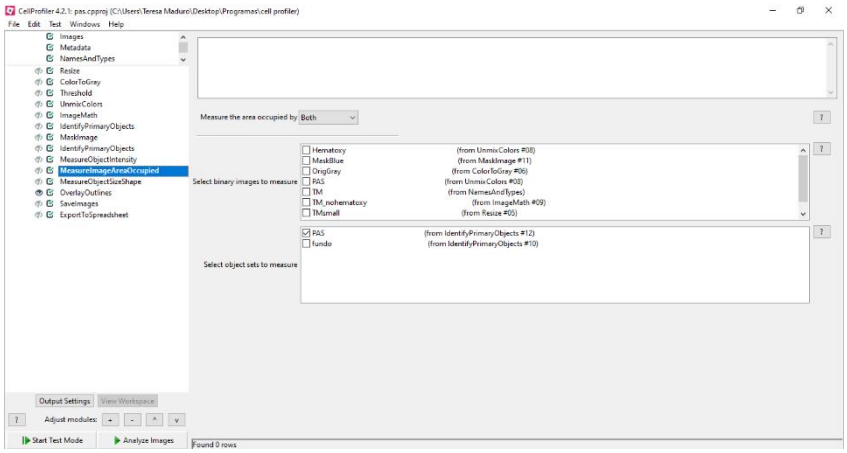

8. Measurement of the stain size and shape

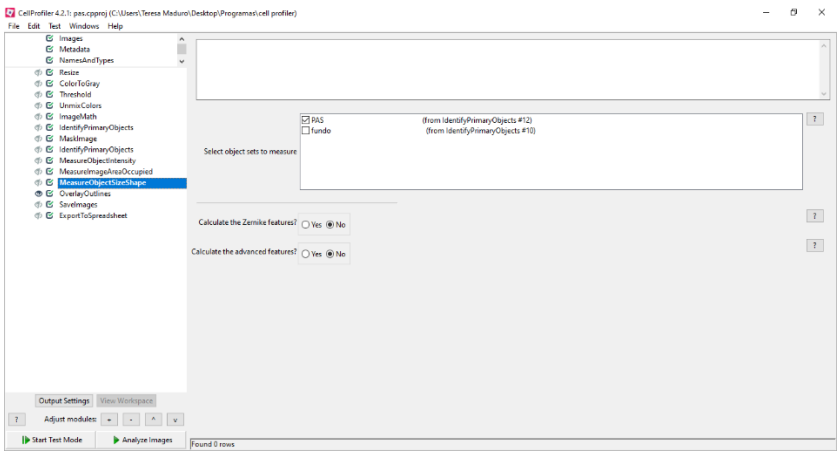

9. Set of the stain outlines

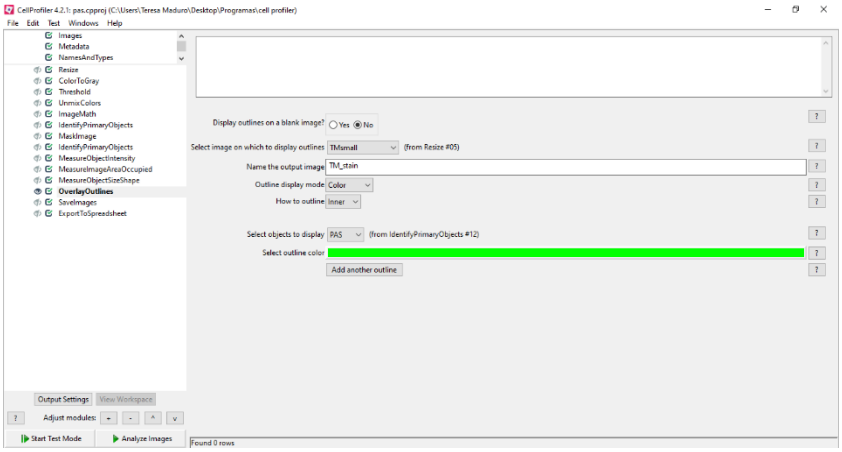

10. Save the images

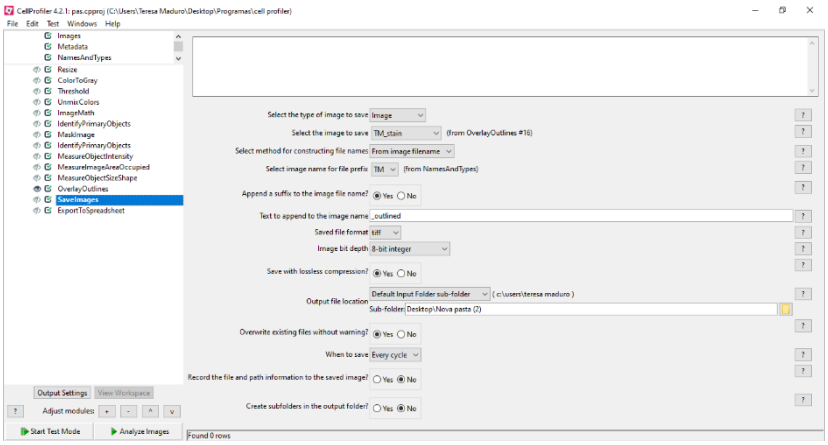

11. Export to the spreadsheet